

5. WONG, M., Y. KANAI, M. MIWA, *et al.* 1983. Immunological evidence for *in vivo* occurrence of a cross-linked complex of poly(ADP-ribose)ated histone H1. *Proc. Natl. Acad. Sci. USA* **80**: 205–209.
6. TAN, E.M. 1989. Antinuclear antibodies: diagnostic markers for autoimmune diseases and probe for cell biology. *Adv. Immunol.* **44**: 93–151.
7. KANAI, Y., M. WATANABE & T. KUBOTA. 2005. Interspecific structural differences in nucleosome as revealed by heteroimmunization in mice with human nucleosome. *Ann. N. Y. Acad. Sci.* **1050**: 89–96.
8. D'ANDREA, M.R. 2003. Evidence linking neuronal cell death to autoimmunity in Alzheimer's disease. *Brain Res.* **982**: 19–30.
9. BECHMANN, I., I. GALEA & I.V.H. PERRY. 2006. What is the blood-brain barrier (not)? *Trends Immunol.* **28**: 5–11.
10. MECCOCI, P., R. EKMAN, L. PARNETTI, *et al.* 1993. Antihistone and anti-dsDNA autoantibodies in Alzheimer's disease and vascular dementia. *Biol. Psychiatry* **34**: 380–385.
11. SEROT, J.M., M.C. BENE, D. CHRISTMANN, *et al.* 1992. Antibodies to chorioid plexus in senile dementia of Alzheimer's type. *J. Clin. Pathol.* **45**: 781–783.
12. MECOCCI P., L. PARNETTI, G. ROMANO, *et al.* 1995. Serum anti-GFAP and anti-S100 autoantibodies in brain aging, Alzheimer's disease and vascular dementia. *J. Neuroimmunol.* **57**: 165–170.
13. D'ANDREA, M.R. 2005. Add Alzheimer's disease to the list of autoimmune diseases. *Med. Hyp.* **64**: 458–463.
14. ZARRABI, M.H., S. ZUCKER, F. MILLER, *et al.* 1979. Immunologic and coagulation disorders in chlorpromazine-treated patients. *Ann. Intern. Med.* **91**: 194–199.
15. SIROTA, P., A.F.A. MICHAEL, S. CLARA, *et al.* 1993. Autoantibodies to DNA in multicase families with Schizophrenia. *Biol. Psychiatry* **33**: 450–455.
16. MELI, E., M. PANGALLO, R. BARONTI, *et al.* 2003. Poly(ADP-ribose) polymerase as a key player in excitotoxicity and post-ischemic brain damage. *Toxicol. Lett.* **139**: 153–162.

Review Article

Strategic targeting of the glucocorticoid receptor for anti-inflammation

Hirotoishi Tanaka * , Noritada Yoshikawa, Noriaki Shimizu,
and Chikao Morimoto

Division of Clinical Immunology and Department of Allergy and Rheumatology, Research Hospital, Institute of Medical Science, University of Tokyo, Tokyo, Japan

Glucocorticoids are produced in the adrenal cortex under the strict control of the hypothalamus-pituitary-adrenal axis and exert a variety of biological actions including the regulation of glucose and lipid metabolism, electrolyte balance, and modulation of the immune, cardiovascular, and central nervous system. Pharmacologically, glucocorticoids are estimated to be used long-term by 0.5-1% of the general population and up to 2.5% of older adults^{1,2)}. Despite the established role of glucocorticoids in controlling short-term inflammation, and despite emerging evidence supporting a disease-modifying role in various autoimmune disorders, concern for adverse events associated with glucocorticoids often limits their use. The glucocorticoid compounds bind the glucocorticoid receptor (GR), which is a member of the nuclear receptor superfamily, and elicit their pharmacological actions. Recent progress in molecular biology of the GR has extended our understanding of their mechanism of action, however, the molecular basis for the side effects have not been fully clarified. Indeed, dissociation of their therapeutic effects and adverse reactions is still one of the most challenging clinical issues to be solved.

In this lecture, I will focus on the recent understanding of the molecular mechanism of glucocorticoid action and our recent work with ursodeoxycholic acid and cortivazol and discuss rationale to develop novel glucocorticoid-like compounds.

Rec.5/17/2007, pp486-493

* Correspondence should be addressed to:

Hirotoishi Tanaka, Division of Clinical Immunology and Department of Allergy and Rheumatology, Research Hospital, Institute of Medical Science, University of Tokyo, 4-6-1 Shirokanedai, Minato-ku, Tokyo 108-8639, Japan. Phone: +81-3-3443-8111, e-mail: hirotnk@ims.u-tokyo.ac.jp

Key words nuclear receptor, transcription, drug, structure

Current Glucocorticoid Therapy

Since the introduction of glucocorticoids in the treatment of rheumatoid arthritis in 1949³⁾, scientists and pharmaceutical com-

panies made intensive efforts to maximize the beneficial and to minimize the side effects of the drug. Many synthetic compounds with glucocorticoid activity were produced and the pharmaco-

Table 1 Classification of the nuclear receptor

	Class I	Class II	Class III
	Steroid hormone receptors	Adopted orphan receptors	Orphan receptors
Representative receptors	Receptors for glucocorticoid (GR), estrogen (ER), progesterone (PR), androgen (AR), mineralocorticoid (MR)	Receptors for thyroid hormone (TR), vitamin D (VDR), all-trans retinoic acid (RAR) and the peroxisome proliferator-activated receptor (PPAR)	SF-1, DAX-1, ERRs, Nurs, CoupTFs, SHP, LRH-1, RORs
DNA binding form	Homodimer	Heterodimer with 9-cis retinoic acid retinoid X receptor (RXR)	Heterodimer with RXR and/or monomer
Response element	Palindrome	Direct repeat	Direct repeat (half site)

logic differences among these chemicals result from structural alterations of their basic backbone and its side groups. These alterations variably affect the bioavailability of these compounds (i.e., gastrointestinal and/or parenteral absorption, plasma half-life, and metabolism, and interaction with the GR). At first, such modification in the structure succeeded in abolishing mineralocorticoid activity in electrolyte handling. On the other hand, modification of physicochemical characteristics (i.e., water solubility/lipophilicity) is considered for parenteral administration or enhancement of topical potency. Most synthetic glucocorticoids (e.g., prednisolone and dexamethasone) are minimally bound to cortisol-binding globulin and circulate mostly bound to albumin, or in the free form.

The side effects occur only with supraphysiologic doses of glucocorticoids and not with proper replacement, which is equivalent to 12 to 15 mg of hydrocortisone/ m² body surface area per day⁹. The side effects of glucocorticoids have been shown to be strictly dose-dependent. Thus, as the dosage is escalated to improve efficacy, the side effects also increase. In addition, some side effects are known to be age- and sex-dependent. Major complications are unlikely with short-term treatment (e.g., less than 2 weeks) with high doses of glucocorticoids, although sleep disturbances and gastric irritation are common complaints, and depression, mania, or psychosis, may be infrequently encountered. On the other hand, many side effects are associated with chronic administration of pharmacologic amounts of glucocorticoids. These side effects include the development of varying degrees of the manifestations of Cushing's syndrome⁴⁻⁶.

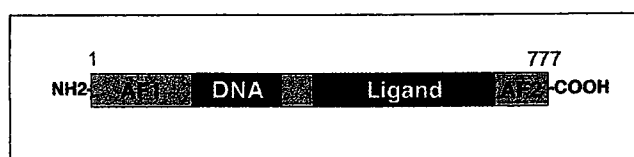


Fig. 1 Primary structure of the human glucocorticoid receptor

GR is A Nuclear Receptor (NR)

NR is a large family of ligand-dependent transcription factors and regulates essential physiological processes including development, reproduction, metabolism, and homeostasis. NRs bind their cognate DNA sequences and modulate gene expression within target tissues. NRs can tentatively be subdivided into three major classes (Table 1). All members of the NR super family share a modular domain structure, consisting of an amino-terminal transcriptional activation function domain (AF1), a conserved zinc-finger DNA binding domain (DBD), a hinge region and a carboxyl-terminal ligand binding domain (LBD) that overlaps with a second transcriptional AF2 domain (Fig. 1). Whereas the AF1 activity is constitutive in most cell types or under tissue-specific regulation, the AF2 activity is strictly ligand-dependent⁷.

The GR LBD, similar to other NR LBDs, is composed of α -helices and β -strands folded into a three-layer helical sandwich. The ligand binding pocket is composed of residues from helices 3, 4, 5, 6, 7, 10, and the AF-2 helix as well as residues from β -strands between helices 5 and 6. Following AF-2 helix is an extended strand that forms a conserved β -sheet with a β -strand

between helices 8 and 9. This C-terminal β -strand also appears to play an important role in receptor activation by stabilizing AF-2 helix in an active conformation. Many AF-2 coactivators for the GR have been identified to date, including steroid receptor coactivator-1 (SRC-1), transcriptional intermediary factor (TIF) 2/GR-interacting protein-1 and cAMP response element binding protein-binding protein (CBP)/p300. These coactivators directly associate with the GR LBD via their LXXLL motif. For example, the LLRYLL sequence in the TIF2 forms a two-turn helix that orients the hydrophobic leucine side chains into a groove formed in part by the AF-2 helix and residues from helices 3, 3', 4, and 5. The N- and C-terminal ends of the coactivator helix are clamped by Glu-755 from the AF-2 helix and Lys-579 in helix 3, respectively. Mutations that disrupt either the first (Glu-755) or the second (Arg-585 and Asp-590) charge clamp dramatically reduce activation mediated by the GR LBD, demonstrating that they are critical for transactivation function of the GR. On the other hand, GR AF-1 coactivators have only recently been described. For example, basal transcription factors including TBP and TFIID have been shown to associate with the AF-1 of GR. TSG101 and DRIP150 have also been reported to interact with GR AF-1 and regulate GR function in a reciprocal manner; GR transcriptional activities are repressed by TSG101 but enhanced by DRIP150. These cofactors are shown to interact with distinct regions of AF-1. Although we now have at hand a large number of regulatory proteins that interact directly or indirectly with the various modular domains of NRs, how ligands differentially regulate the functional interplay between them remains poorly understood⁸⁻¹⁰.

Unlike the GR, most nonsteroidal nuclear receptors like PPAR and RAR can interact with corepressors and repress transcription in the absence of ligand or in the presence of antagonists. These corepressors in turn have histone deacetylase activity that trims acetyl groups of nucleosomes, compacting and silencing the promoter to which unliganded nuclear receptor is bound⁷.

GR-Mediated Anti-inflammation

In the absence of ligand, the GR is retained in the cytoplasm in association with chaperone proteins such as heat shock protein 90 (hsp90). Hormone binding initiates the release of the chaperone proteins and translocation of the receptor into the nucleus where GR binds to DNA promoter elements termed glucocorticoid response element (GRE) from which it can usually activate transcription of the target promoter. A dozens of the target genes of the GR have been identified, most of which transmit metabolic effects of glucocorticoids. A few genes are shown to be

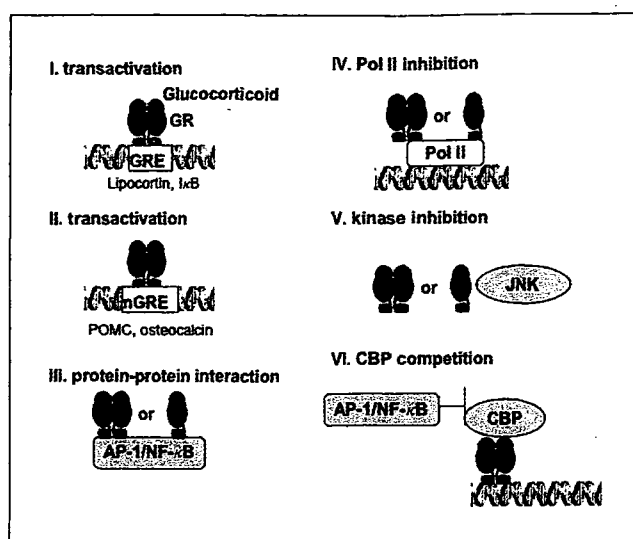


Fig.2 Multiple mechanisms for glucocorticoid receptor (GR)-mediated antiinflammation.

related anti-inflammatory properties of glucocorticoids. On the other hand, transcriptional repression activity is central to the glucocorticoid-mediated anti-inflammation and antiproliferative effects, and a number of transcriptional repression mechanisms mediated by GR have been described (Fig.2). Of note, in contrast to other classes of NR, repression by steroid receptors occurs only in the presence of ligand. The mechanism of repression varies significantly and ranges from effects at the level of DNA to effects on RNA polymerase and transcriptional elongation, and transcription factors directly. These include mechanisms dependent on either GR-DNA or GR-protein interactions. The variety of potential interactions suggests exquisite control over repression that is highly context-dependent. Initial studies emphasized that repression of proinflammatory transcription factors including AP-1 and NF- κ B may be central in GR-mediated anti-inflammation^{8,9}.

Development of Novel Glucocorticoid-like Compounds

Based on the development of molecular biology of the NRs, steroid pharmacology is increasingly focused in the development of novel ligands with selective modulatory activities¹¹. Since dissociation of the side effects of glucocorticoids would definitely contribute to medical fields, GR could be one of the rational molecular targets for such purpose. It is obvious that a novel agent must have the same efficacy in such diseases for which glucocorticoids are currently-indicated, but with reduced side effects. Identification of novel GR ligands have resulted in a

number of divergent terminologies, and Rosen and Miner recently provided putative definitions of some of the key terms¹²⁾:

- SGRM (selective GR modulator) and SeGRA (selective GR agonist). Both SGRM and SeGRA are general class descriptors used to describe compounds with an improved therapeutic index *in vivo* by whatever mechanism.
- Gene-selective compound. This term refers to compounds that act on the receptor to alter gene expression in a gene- or promoter-specific fashion. In other words, some genes might be activated, some might be repressed, but the resulting profile differs from that of currently used glucocorticoids.
- Dissociated compound. This term is usually used to refer to a compound that "dissociates" activation from repression. Compounds in this class fail to globally activate gene expression, but still significantly repress transcription.
- Soft steroids/glucocorticoids (also known as "antedrugs"). This describes corticosteroids that act at or near the site of administration but are inactivated by enzymes, thereby reducing systemic exposure and activity. These are often described for topical and inhaled therapies that act locally but are rapidly metabolized once they enter systemic circulation.

G. Schütz and his colleagues, using dimerization-deficient mutant GR that prevent gene activation by GR but do not affect repression, showed that the anti-inflammatory activity of steroids was maintained and suggested that repression may be sufficient for anti-inflammatory activity¹³⁾. Although a variety of compounds have been tested in terms of dissociation of activation and repression, at this moment a complete dissociated compound is not available. Moreover, such compounds which were once shown to be a dissociated one *in vitro*, often failed to decrease glucocorticoid's metabolic side effects with keeping its anti-inflammatory activities *in vivo*. The other compounds fail to keep their dissociated characteristics at higher, or therapeutic concentrations. Given the battery of genes and the multitude of potential regulatory mechanisms, finding a compound that actually separates all activated genes from all repressed genes seems highly unlikely. It is also unclear whether such a compound would be truly desirable because activation of anti-inflammatory genes may also play a role in the treatment of inflammatory diseases. Of the proposed dissociated compounds that have been published, all have been shown to differentially regulate one or sometimes two genes. This is not the same as demonstrating that the compound is dissociated on all glucocorticoid target genes. It, however, should be noted that the activation/repression hypothesis has provided a very useful framework to find novel compounds with potential utility, and some success has already been achieved

at least preclinically¹²⁾.

Recent structural analyses of the nuclear receptors establish a paradigm of receptor activation, in which agonist binding induces the LBD/AF-2 helix to form a charge clamp for coactivator recruitment¹⁰⁾. However, these analyses have not sufficiently addressed the mechanisms for differential actions of various synthetic steroids in terms of fine tuning of multiple functions of whole receptor molecules. In this line, our studies with two distinct compounds, ursodeoxycholic acid (UDCA) and cortivazol (CVZ), provided the rationale for ligand-based selective modulation of the receptor activities.

Ursodeoxycholic Acid (UDCA)

UDCA is the current mainstay of treatment for various liver diseases including primary biliary cirrhosis, autoimmune hepatitis, and hepatitis C. UDCA has multiple functions, acting not only as a bile secretagogue, but also as a cytoprotective agent, immunomodulator, and inhibitor of cellular apoptosis¹⁴⁻¹⁸⁾. Based on this cumulative evidence of the cytoprotective and immunomodulatory effects of UDCA, we tried to identify the target molecule and pathway of UDCA action. It was shown that UDCA specifically translocates the GR into the nucleus as a DNA binding species but does not elicit its transactivational function in a transient transfection assay (Fig.3). Moreover, the LBD of the GR is responsible for UDCA-dependent nuclear translocation of the GR. Indeed, we demonstrated that UDCA acts on the distinct region of the LBD when compared with the classical GR agonist dexamethasone, resulting in loss of coactivator recruitment and differential regulation of gene expression by the GR (Fig.4). Our data clearly indicated that UDCA, at least in part via activation of the GR, suppresses NF- κ B-dependent transcription through the intervention of GR-p65 interaction^{19,20)}. Together with the established clinical safety of UDCA, we may propose that UDCA could be a prototypical compound for development of a novel and selective GR modifier. Recently, using a fluorescently labeled UDCA molecule, we showed that UDCA shows similar distribution pattern with GR in hepatocytes and that GR is crucial for the nuclear translocation of UDCA for reducing apoptosis²¹⁾. In fact, it is now wellknown that bile acids are ligands of a various NR including the farnesoid X-activated receptor (FXR) and VDR²²⁻²⁵⁾. Our understanding the physiological role of bile acids, thus, is still expanding and NR-target drug development may provide a novel milieu for treatment of various gastrointestinal diseases.

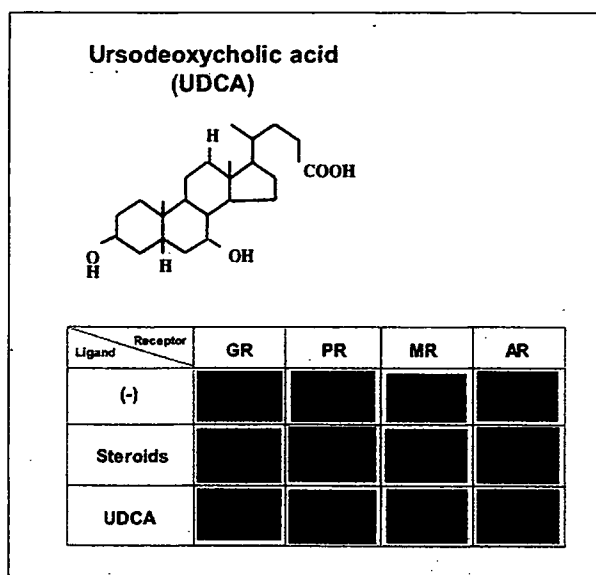


Fig.3 GR-selective activation by ursodeoxycholic acid (UDCA)

Cortivazol (CVZ)

The phenylpyrazologlucocorticoid CVZ is a unique synthetic glucocorticoid agonist with complex binding properties and is more potent than DEX⁶ (Fig.5). We demonstrated that CVZ selectively binds to the GR but not to the MR (Fig. 6) and, based on two criteria, we proposed that the functional interaction of CVZ with the GR LBD is different from that of DEX (Fig.7). Firstly, deletion of the last 12 amino acids of GR severely compromises DEX but not CVZ binding and secondly, the point mutant L753F, in which Leu-753 in AF-2 is substituted to Phe, can efficiently recruit TIF2 to the LBD when bound to CVZ but not when bound to DEX²⁷. These results prompted us to propose that occupancy of the GR LBD by CVZ might lead to a more stable active conformation that can tolerate the disrupting effects of LBD mutations and may have unique effects on the structure and function of the whole GR molecule. Structural docking analysis revealed that although CVZ is more bulky than other agonists, it can be accommodated in the ligand binding pocket of the GR by reorientation of several amino acid side chains but without major alterations in the active conformation of the LBD. In this induced fit model, the phenylpyrazole A-ring of CVZ establishes additional contacts with helices 3 and 5 of the LBD that may contribute to a more stable LBD configuration. Structural and functional analysis revealed that CVZ is able to compensate for the deleterious effects of a C-terminal deletion of the LBD in a manner that mimics the stabilizing influence of the F602S point mutation. CVZ-mediated productive recruitment of

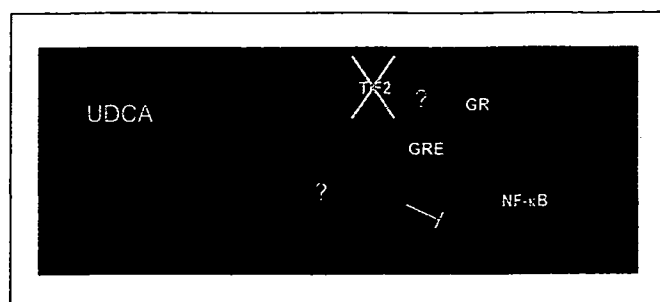


Fig.4 Proposed mechanism of UDCA in GR-mediated immunomodulation

TIF2 to the C-terminally deleted LBD requires the receptor's own DNA binding domain and is positively influenced by the N-terminal regions of GR or progesterone receptor. These results support a model where ligand-dependent conformational changes in the LBD play a role in GR-mediated gene regulation via modular interaction with the DBD and AF-1. Steroid pharmacology is increasingly focused in the development of ligands with selective modulatory activities. Because the mode of interdomain communication may be distinct for each receptor and may be modulated in a ligand-, tissue-, and promoter-context-dependent manner, ligands such as CVZ and other phenylpyrazole analogs that manipulate this regulatory avenue will not only provide a better understanding of the mechanisms of interdomain communication but also provide novel leads in the development of selective GR modulators²⁸. Indeed, a further series of compounds based on an arylpyrazole structure have recently been published. These compounds specifically bind the GR with relatively high affinity. These compounds differ in their relative activity to inhibit cell-based assays of proliferation, adipocyte differentiation or osteoblast differentiation. Moreover, transcriptome profile analyses revealed that the different molecular structures have differential effects on individual target genes. It was striking that, as also indicated in the case of CVZ, subtle changes in structure of the ligand caused markedly distinct GR regulatory effects in more than one cell line. Chromatin immunoprecipitation assays suggested that the different compounds alter the relative affinity of the GR for specific DNA sequences. The authors concluded that the induced structure of the LBD of the GR appears to influence the interaction with DNA sequence and thereby specify a distinct profile of gene regulatory events²⁹. This study overall supports the idea that pursuit of the perfect dissociating glucocorticoid ligand may well be complicated, but it is certainly possible that even an imperfectly dissociating compound may be more than sufficient to offer an improved therapeutic index and thereby

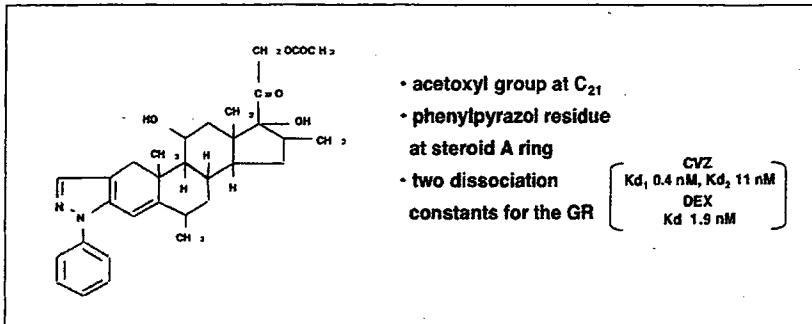


Fig.5 Characteristics of cortivazol (CVZ)

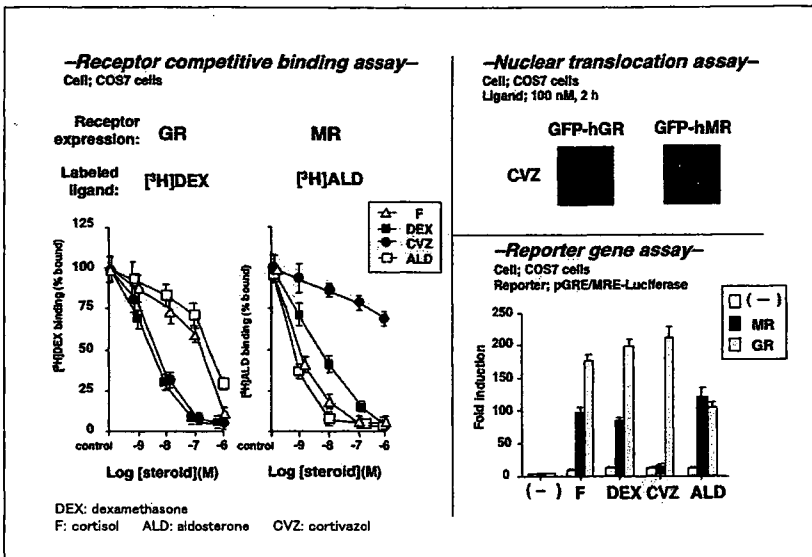


Fig.6 CVZ is a specific ligand for the GR

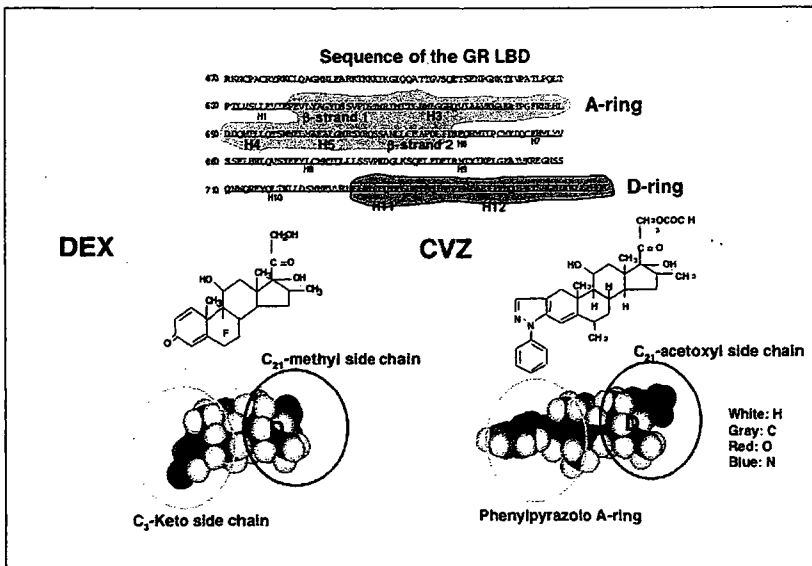


Fig.7 Distinct binding properties of CVZ to the GR -- comparison with dexamethasone (DEX)

unleash the full anti-inflammatory potency of glucocorticoids without the side-effect profile.

Future Directions

A safer glucocorticoid should have full efficacy in anti-inflammatory activity, but reduced efficacy and potency in one or more side effects. The development of new safer anti-inflammatory

agents that target the GR is now gaining momentum after years of work on steroids and, more recently, nonsteroidal molecules. The molecular details behind the action of the newer compounds being described may point the way to more effective assays capable of detecting novel anti-inflammatory agents.

The detection of a tissue selective or a functionally selective ligand for the GR will be difficult, and there is no guarantee, once such a ligand is found, that it will have the necessary profile *in vivo*. However, recent reports of SGRMs with equal efficacy and improved side effect profiles compared with steroids together with molecular discoveries of the receptor mechanism of action provide fertile ground for additional efforts. Thus, despite the difficulties associated with developing a novel glucocorticoid, progress in this area would be a major benefit to the large number of patients suffering from the side effects of steroids, but needing the anti-inflammatory and anti-cancer activity to maintain their quality of life.

Acknowledgement

This work is partially supported by the Grants-in-Aid for Creative Scientific Research 17GS0419 and for Scientific Research (B).

References

- 1) Van Staa TP, Leufkens HG, Abenham L, Begaud B, Zhang B, Cooper C: Use of oral corticosteroids in the United Kingdom. *QJM*, 93: 105-111, 2000.
- 2) Walsh LJ, Wong CA, Pringle M, Tattersfield AE: Use of oral corticosteroids in the community and the prevention of secondary osteoporosis: a cross sectional study. *BMJ*, 313: 344-346, 1996.
- 3) Hench PS, Kendall EC, Slocumb CH, et al: The effect of a hormone of the adrenal cortex (17-hydroxy 11-dehydrocortisone), compound E and of pituitary adrenocorticotrophic hormone on rheumatoid arthritis. *Proc Staff Meet Mayo Clin*, 24: 181-197, 1949.
- 4) Axelrod L: Glucocorticoid therapy. *Medicine*, 55: 39-65, 1976.
- 5) Tyrell JB, Baxter JD: Glucocorticoid therapy. In: Felig P, Baxter JB, Broadus AE (eds), *Endocrinology and Metabolism*, 2nd Edition, McGraw-Hill, New York, 1987, pp788-817.
- 6) Schäcke H, Döcke WD, Asadullah K: Mechanisms involved in the side effects of glucocorticoids. *Pharmacol Ther*, 96: 23-43, 2002.
- 7) Evans RM: The Nuclear Receptor Superfamily: A Rosetta Stone for Physiology. *Mol Endocrinol*, 19(6): 1429-1438, 2005.
- 8) Rhen T, Cidlowski JA: Antiinflammatory Action of Glucocorticoids--New Mechanisms for Old Drugs. *N Engl J Med*, 353: 1711-1723, 2005.
- 9) Buttgereit F, Burmester GR, Lipworth BJ: Optimised glucocorticoid therapy: the sharpening of an old spear. *Lancet*, 365: 801-803, 2005.
- 10) Bledsoe RK, Montana VG, Stanley TB, Delves CJ, Apolito CJ, McKee DD, Consler TG, Parks DJ, Stewart EL, Willson TM, Lambert MH, Moore JT, Pearce KH, Xu HE: Crystal structure of the glucocorticoid receptor ligand binding domain reveals a novel mode of receptor dimerization and coactivator recognition. *Cell*, 110(1): 93-105, 2002.
- 11) Tobin JF, Freedman LP: Nuclear receptors as drug targets in metabolic diseases: new approaches to therapy. *Trends Endocrinol Metab*, 17(7): 284-290, 2006.
- 12) Rosen J, Miner JN: The search for safer glucocorticoid receptor ligands. *Endocr Rev*, 26(3): 452-464, 2005.
- 13) Wintermantel TM, Berger S, Greiner EF, Schutz G: Genetic dissection of corticosteroid receptor function in mice. *Horm Metab Res*, 36(6): 387-391, 2004.
- 14) Brentnall TA: Ursodiol: good drug makes good. *Gastroenterology*, 124(4): 1139-1144, 2003.
- 15) Kowdley KV: Ursodeoxycholic acid therapy in hepatobiliary disease. *Am J Med*, 108(6): 481-486, 2000.
- 16) Hofmann AF: The continuing importance of bile acids in liver and intestinal disease. *Arch Intern Med*, 159(22): 2647-2658, 1999.
- 17) Makino I, Tanaka H: From a choleric to an immunomodulator: historical review of ursodeoxycholic acid as a medicament. *J Gastroenterol Hepatol*, 13(6): 659-664, 1998.
- 18) Sola S, Amaral JD, Aranha MM, Steer CJ, Rodrigues CM: Modulation of hepatocyte apoptosis: cross-talk between bile acids and nuclear steroid receptors. *Curr Med Chem*, 13(25): 3039-3051, 2006.
- 19) Tanaka H, Makino Y, Miura T, Hirano F, Okamoto K, Komura K, Sato Y, Makino I: Ligand-independent activation of the glucocorticoid receptor by ursodeoxycholic acid. Repression of IFN-gamma-induced MHC class II gene expression via a glucocorticoid receptor-dependent pathway. *J Immunol*, 156(4): 1601-1608, 1996.
- 20) Miura T, Ouchida R, Yoshikawa N, Okamoto K, Makino Y, Nakamura T, Morimoto C, Makino I, Tanaka H: Functional modulation of the glucocorticoid receptor and suppression of NF-kappaB-dependent transcription by ursodeoxycholic acid. *J Biol Chem*, 276(50): 47371-47378,

- 2001.
- 21) Sola S, Amaral JD, Castro RE, Ramalho RM, Borralho PM, Kren BT, Tanaka H, Steer CJ, Rodrigues CM: Nuclear translocation of UDCA by the glucocorticoid receptor is required to reduce TGF-beta1-induced apoptosis in rat hepatocytes. *Hepatology*, 42(4): 925-934, 2005.
- 22) Lee FY, Lee H, Hubbert ML, Edwards PA, Zhang Y: FXR, a multipurpose nuclear receptor. *Trends Biochem Sci*, 31(10): 572-580, 2006.
- 23) Huang W, Ma K, Zhang J, Qatanani M, Cu villier J, Liu J, Dong B, Huang X, Moore DD: Nuclear receptor-dependent bile acid signaling is required for normal liver regeneration. *Science*, ;312(5771): 233-236, 2006.
- 24) Chen J, Raymond K: Nuclear receptors, bile-acid detoxification, and cholestasis. *Lancet*, 367(9509): 454-456, 2006.
- 25) LXRS and FXR: the yin and yang of cholesterol and fat metabolism. *Annu Rev Physiol*, 68: 159-191, 2006.
- 26) Schlechte JA, Simons SS Jr, Lewis DA, Thompson EB. [3H] cortivazol: a unique high affinity ligand for the glucocorticoid receptor. *Endocrinology*, 117(4): 1355-1362, 1985.
- 27) Yoshikawa N, Makino Y, Okamoto K, Morimoto C, Makino I, Tanaka H: Distinct interaction of cortivazol with the ligand binding domain confers glucocorticoid receptor specificity: cortivazol is a specific ligand for the glucocorticoid receptor. *J Biol Chem*, 277(7): 5529-5540, 2002.
- 28) Yoshikawa N, Yamamoto K, Shimizu N, Yamada S, Morimoto C, Tanaka H: The distinct agonistic properties of the phenylpyrazolosteroid cortivazol reveal interdomain communication within the glucocorticoid receptor. *Mol Endocrinol*, 19(5): 1110-1124, 2005.
- 29) Wang JC, Shah N, Pantoja C, Meijsing SH, Ho JD, Scanlan TS, Yamamoto KR: Novel arylpyrazole compounds selectively modulate glucocorticoid receptor regulatory activity. *Genes Dev*, 20(6): 689-699, 2006.

Humanized Anti-CD26 Monoclonal Antibody as a Treatment for Malignant Mesothelioma Tumors

Teruo Inamoto,^{1,3} Taketo Yamada,² Kei Ohnuma,¹ Shinichiro Kina,¹ Nozomu Takahashi,¹ Tadanori Yamochi,¹ Sakiko Inamoto,^{1,3} Yoji Katsuoka,³ Osamu Hosono,¹ Hirotohi Tanaka,¹ Nam H. Dang,⁴ and Chikao Morimoto^{1,4}

Abstract Purpose: CD26 is a 110-kDa cell surface antigen with a role in tumor development. In this report, we show that CD26 is highly expressed on the cell surface of malignant mesothelioma and that a newly developed humanized anti-CD26 monoclonal antibody (mAb) has an inhibitory effect on malignant mesothelioma cells in both *in vitro* and *in vivo* experiments.

Experimental Design: Using immunohistochemistry, 12 patients' surgical specimens consisting of seven malignant mesothelioma, three reactive mesothelial cells, and two adenomatoid tumors were evaluated for expression of CD26. The effects of CD26 on malignant mesothelioma cells were assessed in the presence of transfection of CD26-expressing plasmid, humanized anti-CD26 mAb, or small interfering RNA against CD26. The *in vivo* growth-inhibitory effect of humanized anti-CD26 mAb was assessed in human malignant mesothelioma cell mouse xenograft models.

Results: In surgical specimens, CD26 is highly expressed in malignant mesothelioma but not in benign mesothelial tissues. Depletion of CD26 by small interfering RNA results in the loss of adhesive property, suggesting that CD26 is a binding protein to the extracellular matrix. Moreover, our *in vitro* data indicate that humanized anti-CD26 mAb induces cell lysis of malignant mesothelioma cells via antibody-dependent cell-mediated cytotoxicity in addition to its direct anti-tumor effect via p27^{Kip1} accumulation. *In vivo* experiments with mouse xenograft models involving human malignant mesothelioma cells show that humanized anti-CD26 mAb treatment drastically inhibits tumor growth in tumor-bearing mice, resulting in enhanced survival.

Conclusions: Our data strongly suggest that humanized anti-CD26 mAb treatment may have potential clinical use as a novel cancer therapeutic agent in CD26-positive malignant mesothelioma.

Malignant mesothelioma is an aggressive cancer arising from the mesothelial cells lining the pleura. It is usually associated with the history of chronic asbestos exposure (1). Because of the long latency period between asbestos exposure and tumor development, the annual incidence of 2,500 new cases in the

United States is expected to increase by >50% in the coming decade (2). Moreover, incidence world wide is projected to increase substantially in the next decades (3). The prognosis is very poor with a median survival of 4 to 12 months despite the therapies currently used, including surgery, radiotherapy, and chemotherapy (4). Because of the inefficacy of the conventional treatments, novel therapeutic strategies are urgently needed to be developed.

CD26 is a 110-kDa surface glycoprotein with dipeptidyl peptidase IV activity able to cleave selected biological factors to alter their functions (5). CD26/dipeptidyl peptidase IV is involved in T-lymphocyte costimulation and signal transduction processes (6, 7) and regulates topoisomerase II α level in hematologic malignancies, affecting sensitivity to doxorubicin and etoposide (8). Expressed on various tissues (4, 9), CD26 is involved in the development of certain human cancers (9–12). CD26 is also known to serve as a binding motif for extracellular matrix (ECM) in human and rodents (13, 14). Previously, we reported that CD26 was collagen-binding protein using a CD26 positive JM1 cell line, which is derived from malignant mesothelioma (15). Moreover, our previous works have shown that anti-CD26 monoclonal antibody (mAb) inhibits growth of CD26-positive T-cell malignancies (16, 17) and renal cell carcinoma (18).

Authors' Affiliations: ¹Division of Clinical Immunology, Advanced Clinical Research Center, Institute of Medical Science, University of Tokyo and ²Department of Pathology, Keio University, Tokyo, Japan; ³Department of Medicine, Osaka Medical College, Osaka, Japan; and ⁴Department of Hematologic Malignancies, Nevada Cancer Institute, Las Vegas, Nevada

Received 1/16/07; revised 3/14/07; accepted 3/22/07.

Grant support: Ministry of Education, Science, Sports, and Culture grant (K. Ohnuma and C. Morimoto), Ministry of Health, Labor, and Welfare, Japan (C. Morimoto), and Yasuda Medical Foundation (T. Inamoto).

The costs of publication of this article were defrayed in part by the payment of page charges. This article must therefore be hereby marked *advertisement* in accordance with 18 U.S.C. Section 1734 solely to indicate this fact.

Conflict of interest: Dr. Morimoto is a board member of Y's Therapeutics, and Dr. Dang is a scientific adviser in Y's Therapeutics. The other authors have no competing financial interests.

Requests for reprints: Chikao Morimoto, Division of Clinical Immunology, Advanced Clinical Research Center, Institute of Medical Science, University of Tokyo, 4-6-1, Shirokanedai, Minato-ku, Tokyo 108-8639, Japan. E-mail: morimoto@ims.u-tokyo.ac.jp.

© 2007 American Association for Cancer Research.
doi:10.1158/1078-0432.CCR-07-0110

Our previous report shows that the murine anti-CD26 mAb 14D10, which recognizes the cell membrane-proximal glycosylated region starting with a 20-amino acid flexible stalk region of human CD26, has direct antitumor effect by inducing G₁-S arrest while concomitantly blocking the adhesion of cancer cells to the ECM. However, another murine anti-CD26 mAb, termed 5F8, which detects the cysteine-rich domain of CD26, lacks this biological activity (18).

Because human malignant mesothelioma is a highly malignant tumor resistant to apparent conventional treatment, the detection of novel target and development of new treatment strategies in malignant mesothelioma are urgently needed (4, 19). In this report, we analyzed the expression of CD26 in the tissues of patients with malignant mesothelioma and validated the antitumor effect of a novel humanized anti-CD26 mAb which was constructed from high-affinity Fab clone to the 14D10 variable region by targeting malignant mesothelioma, hence concomitantly showing the functional role of CD26 in this neoplasm.

Materials and Methods

Reagents and antibodies. Anti-CD26 mouse mAb (IgG1)14D10, 5F8, and anti-CD45RA mouse mAb (IgG1) 2H4 were developed in our laboratory as described previously (20, 21), with the last one being used as control. Normal human IgG1 (Sigma-Aldrich) was also used as a control. Humanized anti-CD26 mAb (IgG1 isotype) was constructed from 14D10 coding sequence (generously provided by Y's Therapeutics). Mouse mAb to PKB α /Akt, CDK2, CDK4, CDK6, cyclin E, and β -actin were from Cell Signaling Technology Inc., and mouse mAb to p27^{kip1}, p21^{cip1/waf1}, cyclin D1, and activated caspase-3 were from BD Pharmingen. Antihuman IgG, Fc γ fragment specific F(ab')₂ fragment of goat and anti-mouse IgG, Fc γ fragment specific F(ab')₂ fragment of goat were from Jackson ImmunoResearch.

Cell culture and transfection. JMN cells were a kind gift from Dr. Brenda Gerwin (Laboratory of Human Carcinogenesis, NIH, Bethesda, MD). NCI-H2452 and 293T cells were obtained from the American Type Culture Collection. JMN and NCI-H2452 cell lines were derived from patients with malignant mesothelioma. All cells were grown in RPMI medium (Life Technologies Inc.) supplemented with 10% heat-inactivated fetal bovine serum, penicillin (100 units/mL), and streptomycin (100 μ g/mL; Life Technologies) or G418 (500 μ g/mL; Sigma-Aldrich). 293T cells were transfected with full-length CD26 subcloned into a pEB6 vector (22) using FuGENE6 reagent (Roche Diagnostics).

2-(2-methoxy-4-nitrophenyl)-3-(4-nitrophenyl)-5-(2,4-disulfo-phenyl)-2H-tetrazolium assay. Cells were subjected to incubation in 96-well plates in media alone or in the presence of humanized anti-CD26 mAb (0.1, 1.0, or 10 μ g/mL) or 2H4 (0.1, 1.0, or 10 μ g/mL) for a total volume of 100 μ L (5×10^3 cells per well). After 24 h of incubation in 37°C, 2-(2-methoxy-4-nitrophenyl)-3-(4-nitrophenyl)-5-(2,4-disulfo-phenyl)-2H-tetrazolium (Seikagaku) was added to each well. After another 2 h of incubation, water soluble formazan dye upon bioreduction in the presence of an electron carrier, 1-methoxy-5-methylphenazinium, was measured at 450 nm using a microplate reader (Bio-Rad). All samples were tested in triplicate. Values reported represent the means of triplicated wells, and SE was within 15.

Immunohistochemistry. For immunohistochemistry, 12 patients' surgical specimens consisting of seven malignant mesothelioma, three reactive mesothelial cells, and two adenomatoid tumors were evaluated. For each, 10% formalin-fixed, paraffin-embedded specimens, containing both the carcinoma and its adjacent nonneoplastic tissue, were prepared. Paraffin-embedded tissues were dewaxed and rehydrated

using xylene and ethanol, respectively. Slides were deparaffinized, then heated in a microwave processor for antigen retrieval in 10 mmol/L citrate buffer (pH 6.0) for 10 min. After blocking in 3% (v/v) bovine serum albumin, slides were incubated at 4°C overnight with the primary antibody (anti-CD26 mAb) and washed with PBS and the secondary antibody was labeled with biotin and applied for 30 min. Streptavidin-LSA amplification method was carried out for 30 min followed by peroxidase/diaminobenzidine substrate/chromagen. The slides were counterstained with hematoxylin. Two different pathologists checked the validity of the obtained results. All human specimens were obtained from Department of Pathology, Keio University (Tokyo, Japan), and informed consents were obtained from all patients according to the format of the institutional review board.

Depletion of endogenous CD26. To deplete endogenous CD26, small interfering RNA (siRNA) oligo-targeting CD26 cDNA (accession no. NM_001935) was made according to the design site of TAKARA BIO;⁵ sense: 5'-GAAAGGUGUCAGUACUAAU TT-3', antisense: 3'-TT CUUUCACAGUCAUGAUAA-5', with scrambled control of small interfering RNA oligo-targeting human Cas-L; sense: 5'-UAAUAGG-GUCGGGUAAC TT-3', antisense: 3'-TT AUUAAUCCAGCCCA-UUUG-5' being used as control. CD26 siRNA oligo (siCD26) was transfected using TransIT-TKO transfection reagent (Mirus Bio Corporation) according to the manufacturer's protocol.

SDS-PAGE and immuno-blotting. Preparation of whole-cell lysates, cell fractionations, and SDS-PAGE were done as described elsewhere (23).

Antibody-dependent cell-mediated cytotoxicity. The capacity of mAb to induce effector cell-dependent lysis of tumor cells was evaluated in Calcein-AM-release assay. Healthy donor natural killer cells were isolated from peripheral blood mononuclear cells by NK Cell Isolation kit II Miltenyi Biotec (Bergisch Gladbach) and used as effector cells. Target cells (1×10^6) were labeled with 10 μ mol/L Calcein-AM (Dojindo) under shaking conditions at 37°C for 1 h. Cells were washed thrice with PBS and were resuspended in culture medium (1×10^5 cells/mL). Labeled cells were dispensed in 96-well U-bottomed plates (5×10^3 in 50 μ L/well) and preincubated (37°C, 30 min) with 50 μ L of 7-fold serial dilutions of humanized anti-CD26 mAb or 14D10 in culture medium, ranging from 0.1 pg/mL to 0.1 mg/mL (final concentrations). Culture medium was added instead of mAb to determine the spontaneous Calcein-AM release, with Triton X-100 (1% final concentration) being added to determine the maximal Calcein-AM release. Thereafter, human effector cells (HuEC) were added to the wells (5×10^5 cells per well) and cells were incubated at 37°C overnight. Supernatants were then collected for measurement of the Calcein-AM release. Percentage of specific lysis was calculated using the following formula: % specific lysis = (experimental release - spontaneous release)/(maximal release - spontaneous release) \times 100; where maximal release was determined by adding Triton X-100 to target cells and spontaneous release was measured in the absence of sensitizing Abs and effector cells.

Complement-dependent cytotoxicity. Complement-dependent cytotoxicity (CDC) assay was done as described previously (24). Target cells were dispensed in 96-well U-bottomed plates (1×10^5 cells per well) incubated with various concentrations of mAbs at 4°C for 30 min. Subsequently, human serum was added and cells were incubated at 37°C for 2 h. Evaluation of CDC-specific cell death along with antibody-dependent cell-mediated cytotoxicity (ADCC)-specific cell death was assessed by Annexin V-FITC Apoptosis Detection kit (BioVision) and detection of activated caspase-3.

Assessment of antitumor activity of humanized anti-CD26 mAb in effector-depleted SCID mice. All *in vivo* studies were approved by the Institute Animal Care and Use Committee. Six-week-old female NOD-SCID mice were purchased from Charles River (Kanagawa, Japan) and were pretreated with anti-asialo-GM1 polyclonal antisera 25% (v/v; WAKO) i.p. 1 day before mAb treatment.

⁵ <http://www.takara-bio.co.jp/RNAi.htm>

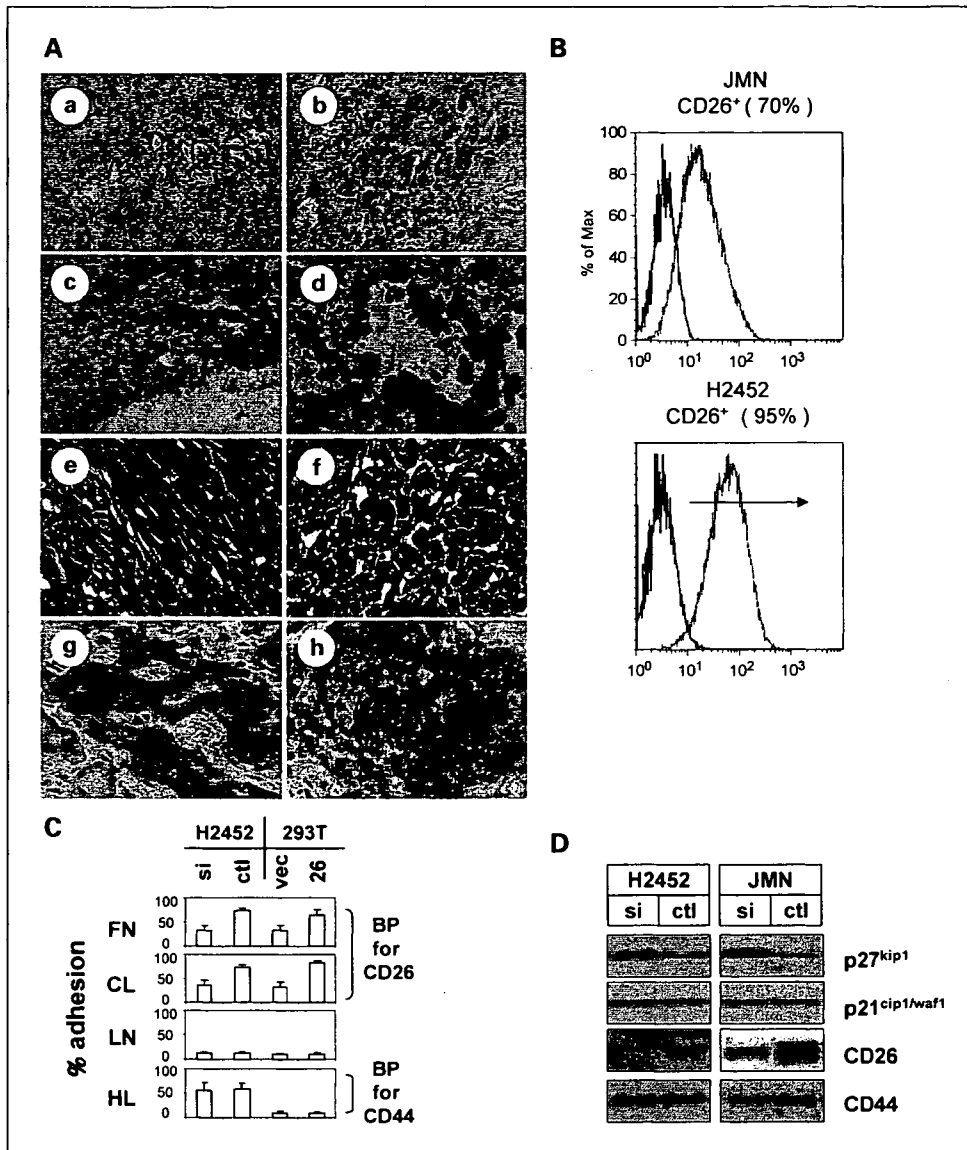


Fig. 1. Expression and functional role of CD26 in malignant mesothelioma. **A**, immunohistochemical localization of CD26 in adenomatoid tumor, reactive mesothelial cells and malignant mesothelioma. *a*, CD26 in adenomatoid tumor; *b*, CD26 in reactive mesothelial cells; *c*, CD26 in localized malignant mesothelioma; *d*, CD26 in well-differentiated papillary malignant mesothelioma; *e* and *f*, H&E stain in diffuse malignant mesothelioma; *g* and *h*, CD26 in diffuse malignant mesothelioma. Diffuse malignant mesothelioma specimens are showing biphasic features of sarcomatous malignant mesothelioma (*f, h*) and epithelial malignant mesothelioma (*g, i*). Indicated panels are representative of 12 consecutive specimens. Original magnification, $\times 100$. **B**, surface expression of CD26 on mesothelioma cell lines was analyzed by flow cytometry. Gray line, CD26 histograms were obtained by staining mouse anti-CD26mAb (14D10) followed by staining with rabbit anti-mouse IgG FITC conjugate; black line, control histograms represent back ground fluorescence obtained by staining of isotype-matched control mAb (2H4). **C**, adhesive property of CD26 to ECM. CD26-depleted NCI-H2452 (*si*), scrambled control oligo-transfected NCI-H2452 (*ctl*), pEB6 vector – transfected 293T (*vec*), or pEB6-CD26 – transfected 293T (26) were plated onto 60-mm dishes (2×10^6 cells per dish) coated with fibronectin (*FN*), collagen I (*CL*), laminin (*LN*), or hyaluronan (*HL*) and cultured for 18 h. Fibronectin and collagen I are binding proteins (*BP*) to extracellular region of CD26, with hyaluronan being binding protein for CD44. The adhesive ability of cancer cells was expressed as the mean number of cells that had attached to the bottom surface of the dish. Columns, number of cells per field of view; bars, SD. Values for adhesion were determined by calculating the average number of adhesive cells per squared millimeters over three fields per assay and expressed as an average of triplicate determinations. Adhesive cells (%): adhesive cells/adhesive cells + nonadhesive cells. **D**, depletion of CD26 elicits up-regulation of p27^{kip1}. NCI-H2452 cells and JMN cells were transfected with siRNA oligo (*si*) of CD26 or control oligo (*ctl*). At 48 h after transfection, cells were harvested, lysed, and subjected to SDS-PAGE, then probed by specific antibody to p27^{kip1}, p21^{cip1/waf1}, CD26, and CD44.

To assess the effect of humanized anti-CD26 mAb against tumorigenicity, JMN cells (1×10^6) were inoculated s.c. into the left flank of mice. Mice were treated with intratumoral injection of isotype-matched control mAb and 5F8, 14D10, or humanized anti-CD26 mAb (10 μ g per each injection) on the 14th day after cancer cell inoculation when the tumor mass became visible (5 mm in size). Each mAb was given thrice per week. Tumor-bearing mice were then monitored for tumor development and progression. Tumor size was determined by caliper measurement of the largest (*x*) and smallest (*y*)

perpendicular diameters and was calculated according to the formula $V = \pi/6 \times xy^2$.

To assess the effect of humanized anti-CD26 mAb against tumor dissemination, JMN cells (1×10^5) were injected i.v. via tail vein. Thereafter, mice were treated with i.v. injection of isotype-matched control mAb and 5F8, 14D10, or humanized anti-CD26 mAb (10 μ g per each injection), starting on the day of cancer cell injection. Each mAb was given thrice per week. Cumulative proportion survival was assessed by Kaplan-Meier.

Table 1. CD26 expression profile in patient samples

Patient no.	Gender/Age	Origin	Histology	CD26	
				CS	C
1	M/55	Pleura	RMC	-	±
2	F/63	Pleura	RMC	-	±
3	M/58	Pleura	RMC	-	±
4	F/39	Ovary	AT	-	+
5	F/5	Ovary	AT	-	±
6	M/67	Pleura	MM	+	++
7	M/60	Pleura	MM	++	+++
8	M/49	Pleura	MM	+	++
9	F/74	Pleura	MM	-	++
10	M/50	Pleura	MM	++	++
11	M/77	Pleura	MM	+	+++
12	M/61	Pleura	MM	+	+++

Abbreviations: RMC, reactive mesothelial cell; AT, adenomatoid tumor; MM, malignant mesothelioma; CS, cell surface; C, cytoplasm.

Assessment of antitumor activity of humanized anti-CD26 mAb in effector-present Balb mice. Six-week-old female Balb mice were purchased from Charles River, and treatment with anti-asialo-GM1 polyclonal antisera was not introduced to preserve the binding of the mouse effector system.

To assess the effect of humanized anti-CD26 mAb against tumorigenicity, JMN cells (1×10^6) were inoculated s.c. into the left flank of mice. Mice were treated with intratumoral injection of isotype-matched control mAb and 5F8, 14D10, or humanized anti-CD26 mAb (10 μ g per each injection) on the 14th day after cancer cell inoculation when the tumor mass became visible (5 mm in size). Each mAb was given thrice per week. Tumor-bearing mice were then monitored for tumor development and progression. Tumor size was determined by caliper measurement of the largest (x) and smallest (y) perpendicular diameters and was calculated according to the formula $V = \pi/6 \times xy^2$. On the 35th day after the first mAb treatment, all mice were euthanized to assess the microscopic feature of resected specimens in s.c. tumorigenicity model.

To assess the effect of humanized anti-CD26 mAb against tumor dissemination, JMN cells (1×10^5) were i.v. injected via tail vein. Thereafter, mice were treated with i.v. injection of isotype-matched control mAb or humanized anti-CD26 mAb (10 μ g per each injection) starting on the day of cancer cell injection. Each mAb was given thrice per week. Cumulative proportion of survival was assessed by Kaplan-Meier. To further assess the effect of humanized anti-CD26 mAb on distant metastasis formation, treated mice were euthanized and multiple metastasis formation in the lung and liver was calculated in another tumor dissemination model. JMN cells (1×10^5) were injected i.v. into mice in each group. Mice were treated with i.v. injection of isotype-matched control mAb (lane 1, n = 4), 5F8 (lane 2, n = 4), 14D10 (lane 3, n = 4), or humanized anti-CD26 mAb (lane 4, n = 4) on the day of cancer cell injection. Each mAb was given thrice per week. On the 35th day after cancer cell injection, mice were euthanized and multiple metastasis formation in the lung and liver was calculated.

Construction of HuEC-engrafted mice and assessment of antitumor activity in NOD/Shi-scid. IL-R γ ^{null} mice. NOD/Shi-scid. IL-R γ ^{null} (NOG mice) were obtained from Central Institute for Experimental Animals. Human peripheral blood mononuclear cells were isolated from the peripheral blood of a healthy donor using Lymphoprep (AXIS-SHIELD) and were used as HuEC. Thereafter, HuEC (5×10^5 cells) were injected i.p. in a volume of 0.2 mL suspended in PBS into NOG-SCID mice under sterile conditions. The mice were pretreated with a 0.2 mL

anti-asialo-GM1 polyclonal antisera 25% (v/v; WAKO) given i.p. 1 day before HuEC injection. NCI-H2452 cells (5×10^4) were injected i.p. into SCID mice engrafted with human HuEC 1 day after HuEC injection. One, three, and five days later, humanized anti-CD26 mAb were injected i.p. Mice were observed daily to monitor for death due to ascites tumor development. Cumulative proportion of survival was assessed by Kaplan-Meier.

Results

Cell surface CD26 is highly expressed on human malignant mesothelioma. We first evaluated CD26 expression level on surgically resected human malignant mesothelioma tissues from patients. Twelve consecutive surgically resected specimens from the primary sites were examined for cell surface CD26 expression. CD26 was highly expressed on all malignant mesothelioma tissues (Fig. 1A; Table 1). In adenomatoid tumor or reactive mesothelial cells, CD26 expression was very weak (Fig. 1A-a,b). In contrast, CD26 was highly expressed in various pathologic types of malignant mesothelioma, including localized malignant mesothelioma, well-differentiated papillary malignant mesothelioma, and diffuse malignant mesothelioma (Fig. 1A-c to h). These results suggested that CD26 is highly expressed in malignant mesothelioma but not in benign mesothelial tissues.

CD26 plays a role in cell adhesion to ECM. Malignant mesothelioma cell lines, JMN and NCI-H2452, exhibited high-surface CD26 expressions (Fig. 1B).

Because CD26 has been described previously to play a role in cell adhesion to the ECM proteins (13, 25), we examined whether CD26 plays a role in cellular interaction with the ECM. As seen in Fig. 1C, NCI-H2452 that were depleted of endogenous CD26 using siRNA oligo showed significant loss of CD26 binding to ECM proteins, including fibronectin and collagen I. In contrast to these results, depletion of CD26 did not alter binding to laminin (an ECM protein lacking binding ability to CD26) or hyaluronan (a ligand for CD44; Fig. 1C). In further support of these findings, 293T cells transfected with full-length CD26 cDNA subcloned into pEB6 vector showed higher binding ability to fibronectin and collagen I than control pEB6-transfected 293T cells (Fig. 1C). Moreover, depletion of CD26 was associated with the up-regulation of p27^{kip1} (Fig. 1D). These findings thus suggested that CD26 serves as a binding molecule to distinct ECM proteins and that contact inhibition may play a contributing role to the observed CD26 depletion-mediated up-regulation of p27^{kip1} associated with CD26 depletion (26, 27).

Anti-CD26 mAb perturbs cellular binding to ECM. Because CD26 proved to be an ECM-binding protein, we further evaluated whether anti-CD26 mAbs disrupt cellular adhesion to ECM. For this purpose, isotype-matched control mAb and 5F8, 14D10, and humanized anti-CD26 mAb were evaluated for potential disruption to cellular adhesion to ECM. As seen in Fig. 2A, JMN cells treated with 14D10 and humanized anti-CD26 mAb had decreased binding to fibronectin and collagen I, whereas control mAb and 5F8 (anti-CD26 mAb without biological function) did not influence binding to fibronectin and collagen I. Moreover, 14D10 and humanized anti-CD26 mAb transmitted direct growth inhibition to JMN cells by *in vitro* proliferation assay in a dose-dependent manner, with humanized anti-CD26 mAb having a stronger antiproliferative

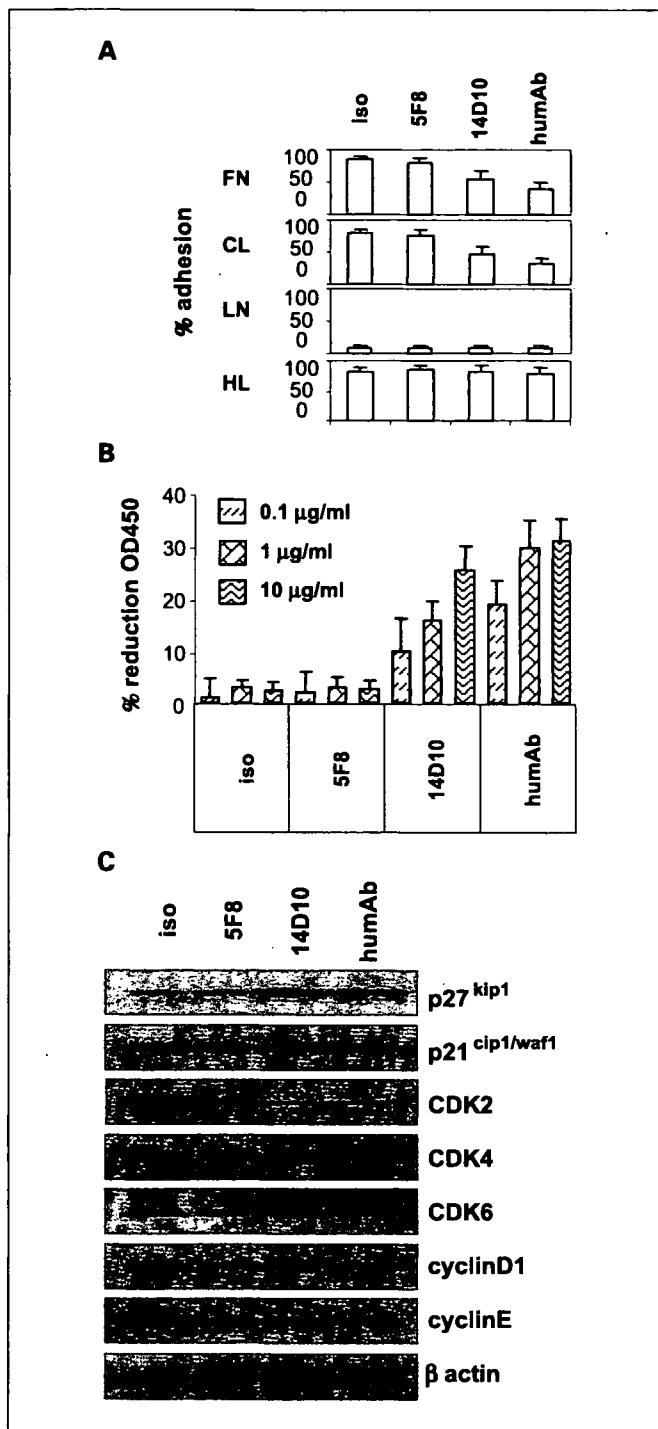


Fig. 2. Inhibitory effect of anti-CD26 mAbs on malignant mesothelioma proliferation. **A.** effect of anti-CD26 mAb on cell adhesion to ECM. JMN cells treated with isotype-matched control mAb (*iso*), 5F8, 14D10, or humanized anti-CD26 mAb (*humAb*) were plated onto 60-mm dishes (2×10^6 cells per dish) coated with fibronectin, collagen I, laminin, or hyaluronan and cultured for 18 h. Adhesive cells (%): adhesive cells/adhesive cells + nonadhesive cells. **B.** 5×10^3 cells per well of JMN were incubated in 96-well plates in the presence of either isotype-matched control mAb, 5F8, 14D10, or humanized anti-CD26 mAb. After 24 h of antibody treatment, water-soluble formazan dye upon bioreduction in the presence of an electron carrier, 1-methoxy-5-methylphenazinium, was measured at 450 nm using a microplate reader as described in Materials and Methods, and growth inhibitory ratio was calculated as percentage reduction of absorbance 450 nm. **C.** JMN cells were treated with isotype-matched control mAb, 5F8, 14D10, or humanized anti-CD26 mAb. At 18 h after antibody administration, cells were harvested, lysed, and subjected to SDS-PAGE, then probed by specific antibody to p27^{kip1}, p21^{cip1/waf1}, CDK2, CDK4, CDK6, cyclinD1, cyclinE, and β -actin.

effect than 14D10 (Fig. 2B). Importantly, 14D10 and humanized anti-CD26 mAb induced up-regulation of p27^{kip1} and down-regulation of CDK2. These results suggested that both 14D10 and humanized anti-CD26 mAb dynamically transmit contact inhibition-related growth inhibition via up-regulation of p27^{kip1} and down-regulation of CDK2.

Humanization of anti-CD26 mAb results in ADCC. Whereas both 14D10 and humanized anti-CD26 mAb had similar direct effect on cancer cells, our present studies emphasized the different biological effects of humanized anti-CD26 mAb compared with 14D10 through the use of ADCC assay with HuEC. When effector/target (E/T) ratio was held constant at 50, JMN cells treated with humanized anti-CD26 mAb showed specific lysis via ADCC in an antibody dose-dependent manner (Fig. 3A, left). Importantly, JMN cells treated with 14D10 did not show ADCC-specific lysis (Fig. 3A, left), suggesting that humanization of 14D10 to humanized anti-CD26 mAb results in the induction of potent ADCC activity via engagement of the human effector system. Moreover, as seen in Fig. 3A (right), humanized anti-CD26 mAb provoked ADCC-specific lysis in effector-dose-dependent manner. These results were also found when other CD26 positive malignant mesothelioma line besides JMN (NCI-H2452) was used as target cells (Table 2). These data suggested that humanized anti-CD26 mAb possesses a novel biological function other than the direct effect on target cells seen with 14D10, namely ADCC-specific lysis. To better characterize the humanized anti-CD26 mAb-mediated ADCC, apoptosis assays using propidium iodide-annexin V staining and detection of cleaved caspase-3 were used. In these assays, cross-linking method using anti-human IgG, Fc γ fragment specific F(ab')₂ fragment of goat, and anti-mouse IgG, Fc γ fragment specific F(ab')₂ fragment of goat were used as mimicry of human effectors to humanized anti-CD26 mAb and 14D10, respectively. As seen in Fig. 3B (top three panels), cross-linked humanized anti-CD26 mAb induced late apoptosis, whereas cross-linked 14D10 did not induce late and early apoptosis. Importantly, neither humanized anti-CD26 mAb nor 14D10-induced CDC using human complement (Fig. 3B). To further support these binding, only cross-linked humanized anti-CD26 mAb induced activation of caspase-3 in JMN cells, whereas neither cross-linked 14D10, humanized anti-CD26 mAb plus human complement, and 14D10 plus human complement induced activation of caspase-3 (Fig. 3C). These results therefore indicated that humanized anti-CD26 mAb elicits ADCC-specific lysis but not CDC-specific lysis.

Humanized anti-CD26 mAb possesses direct in vivo anti-tumor effect on malignant mesothelioma cells. Because we recently showed that 14D10 exhibits direct in vivo antitumor effect on solid tumors (24), we further examined whether humanized anti-CD26 mAb has similar in vivo antitumor effect. For this purpose, we used NOD-SCID mice, which lack functional B and T cells as well as most natural killer cell activity (28). To minimize the effect of mouse effector cells, NOD-SCID mice were pretreated by anti-asialo-GM1 polyclonal antisera before being subjected to humanized anti-CD26 mAb functional evaluation. As seen in Fig. 4A and B, humanized anti-CD26 mAb and 14D10 reduced the tumorigenicity of s.c. inoculated JMN, with humanized anti-CD26 mAb being more potent in reducing tumor formation. These observed results suggested that humanized anti-CD26 mAb possesses stronger direct antitumor effect than 14D10. To

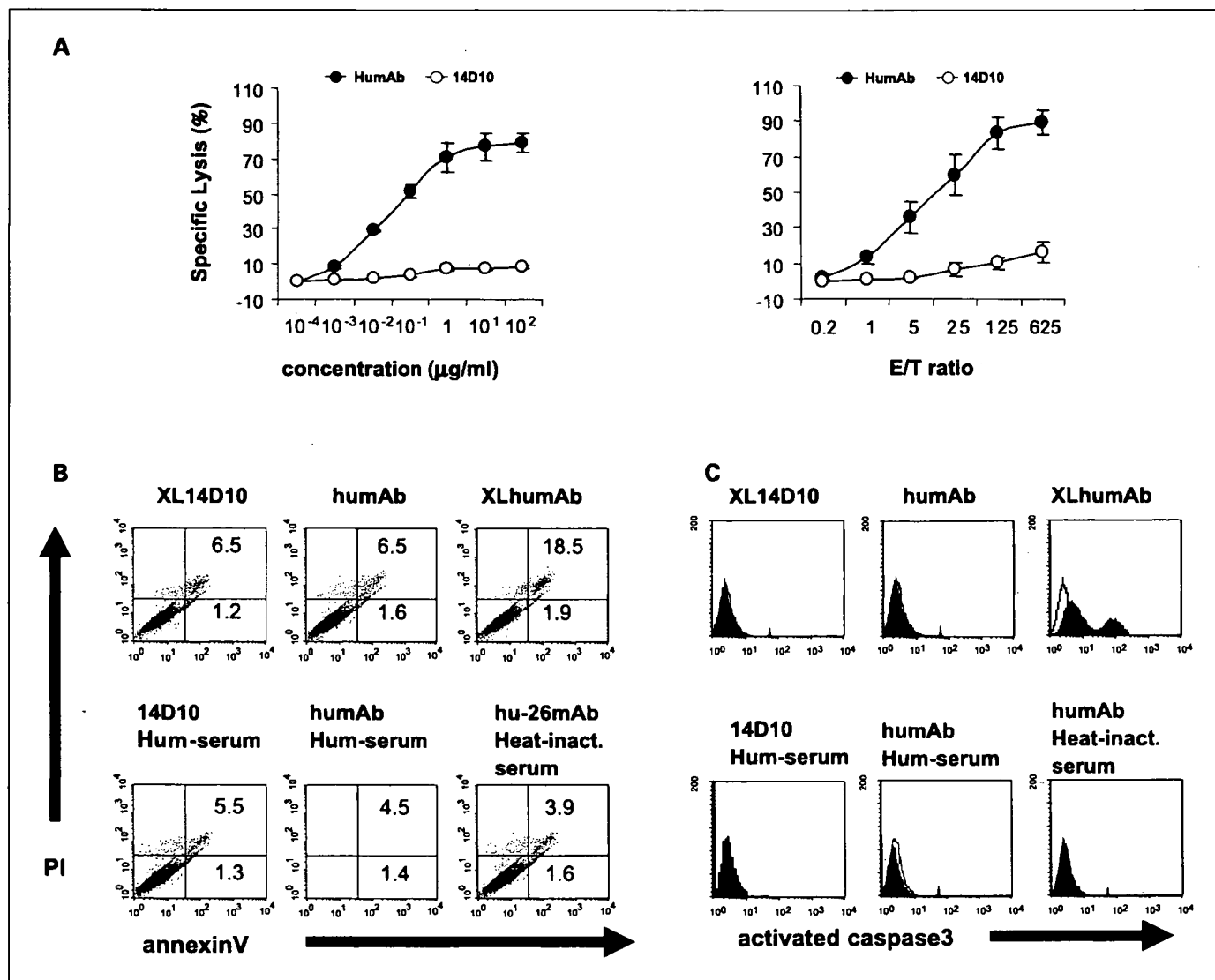


Fig. 3. ADCC-specific lysis of JMN cells by humanized anti-CD26 mAb. *A*, ADCC of humanized anti-CD26 mAb and 14D10 at the indicated concentrations on the X axis were examined (left). Effector/target (E/T) ratio was held constant at 50. ADCC of humanized anti-CD26 mAb and 14D10 in the presence of varying effector/target ratios were examined (right). Concentrations of mAbs were held constant at 5 µg/mL. Natural killer cells from healthy donor were used as effector cells. *B*, as a mimicry of effector cells in ADCC effects, cross-linking (XL) method of humanized anti-CD26 mAb and 14D10 was used. Top, cross-linked 14D10, intact humanized anti-CD26 mAb, cross-linked humanized anti-CD26 mAb, respectively. To examine the CDC, human serum was used. Bottom, 14D10 with serum, humanized anti-CD26 mAb with serum, and humanized anti-CD26 mAb with heat-inactivated serum. X axis, annexin V; Y axis, propidium iodide (PI). *C*, activated caspase-3 was evaluated in JMN cells pretreated with the cross-linked 14D10, intact humanized anti-CD26 mAb, cross-linked humanized anti-CD26 mAb, respectively (top), or in JMN cells pretreated with the 14D10 plus serum, humanized anti-CD26 mAb plus serum, and humanized anti-CD26 mAb plus heat-inactivated serum, respectively (bottom). X axis, activated caspase 3, Y axis, relative cell markers.

further examine the direct antitumor activity of humanized anti-CD26 mAb on tumor dissemination, we examined the effect of i.v.-given antibodies in a JMN xenograft model. As seen in Fig. 4C, humanized anti-CD26 mAb and 14D10 enhanced mouse survival when both antibodies were given i.v., with humanized anti-CD26 mAb being more efficient in promoting survival. All together, these observed results suggested that humanized anti-CD26 mAb is more potent than 14D10 in its direct antitumor activity.

Mouse effector system may potentiate antitumor effect of anti-CD26 mAb. While both humanized anti-CD26 mAb and 14D10 showed direct *in vivo* antitumor effect, we next examined the potential involvement of mouse effector system in anti-CD26 mAb activity induced antitumor effect. For this

purpose, we used Balb mice which possess robust natural killer cell activity. As seen in Fig. 5A, humanized anti-CD26 mAb and 14D10 reduced the tumorigenicity of s.c.-inoculated JMN. It should be noted that both 14D10 and humanized anti-CD26 mAb reduced tumor formation in the presence of mouse effector system (Fig. 5A). As seen in Fig. 5B, both humanized anti-CD26 mAb and 14D10-treated tumors showed resultant dead tissues upon microscopic analyses. These results suggested that both humanized anti-CD26 mAb and 14D10 used the mouse effector system in marked contrast with the observed differences between humanized anti-CD26 mAb and 14D10 in a mouse effector-depleted xenograft model. Additional studies using i.v. administration of JMN cells showed that i.v. injection of humanized anti-CD26 mAb effectively enhanced mouse

Table 2. Specific lysis by humanized anti-CD26 mAb in human malignant mesothelioma lines

MFI	JMN	NCI-H2452
CD26	68	56
% ADCC lysis	67	65

Abbreviations: MFI, mean fluorescent intensity; % ADCC lysis, percentage of ADCC-specific lysis.

survival in the presence of mouse effector system (Fig. 5C). Importantly, formation of distant JMN was similarly inhibited by both humanized anti-CD26 mAb and 14D10 (Fig. 5D). These data indicated that mouse effector system potentiates the anti-CD26 mAb-mediated direct antitumor effect.

Human effector system may potentiate antitumor effect of humanized anti-CD26 mAb. We next evaluated the potential involvement of human effector system in anti-CD26 mAb induced antitumor effect. For this purpose, NOG mice which have significant defects in T, B, and natural killer cell activities were used in a NCI-H2452 xenograft model construction. Human peripheral blood mononuclear cells were used as HuEC in this *in vivo* model. To completely deplete mouse effector system, NOG mice were pretreated with anti-asialo-GM1 antisera 1 day before i.p. HuEC implantation. As seen in Fig. 6, i.p. administration of humanized anti-CD26 mAb drastically enhanced NCI-H2452 xenograft mouse survival in the absence of HuEC. It should be noted that while 14D10 also enhanced mouse survival, its effect was much weaker than humanized anti-CD26 mAb in the absence of HuEC (Fig. 6). These results suggested that humanized anti-CD26 mAb possesses stronger direct antitumor effect. Importantly, in the presence of HuEC, the antitumor effect of humanized anti-CD26 mAb was exaggerated, whereas the antitumor effect of 14D10 was not altered significantly (Fig. 6). All together these observed results suggested that CD26 is an appropriate molecular target for mesothelioma therapy and humanized anti-CD26 mAb regulates tumor growth by at least two distinct mechanisms of action through its direct antitumor activity, as well as its ability to engage human effector system.

Discussion

In this study, we show the antitumor effect of anti-CD26 mAb in an *in vitro* and *in vivo* model. Importantly, our study suggests that humanization of anti-CD26 mAb yields additive antitumor effect to contact inhibition associated with p27^{kip1} induction. Our study also indicates the functional role of CD26 as a binding protein to ECM in human malignant mesothelioma.

Immunohistologic analysis indicates that human malignant mesothelioma cells express high level of surface CD26 than nonmalignant tissue, suggesting that CD26 may play a role in cancer growth and progression. It should be noted that depletion of endogenous CD26 in NCI-H2452 using siRNA oligo results in significant loss of binding to ECM, including fibronectin and collagen I. Moreover, 293T cells transfected with full-length CD26 cDNA exhibit higher binding affinity to fibronectin and collagen I than control mock-transfected 293T

cells. Moreover, depletion of CD26 leads to the up-regulation of p27^{kip1}. These findings thus suggest that CD26 is involved in cancer cell adhesion to ECM and that contact inhibition may play a contributing role to the observed CD26 depletion-mediated up-regulation of p27^{kip1}. Of note is the fact that it has

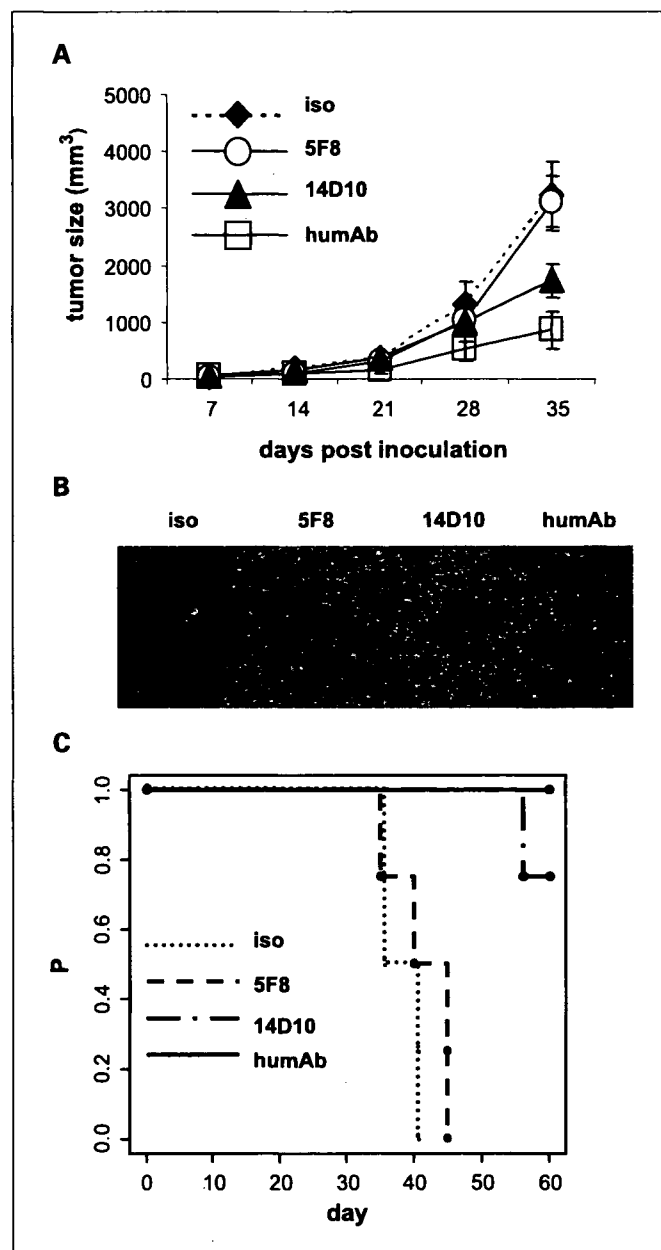


Fig. 4. *In vivo* direct effect of humanized anti-CD26 mAb: ADCC depletion model. Six-week-old female NOD-SCID mice were pretreated with anti-asialo-GM1 polyclonal antisera 1 d before treatment. **A**, effect of humanized anti-CD26 mAb in s.c. tumorigenicity was evaluated. JMN cells (1×10^6) were inoculated s.c. into the left flank of mice. Mice were treated with intratumoral injection of isotype-matched control mAb ($n = 4$), 5F8 ($n = 4$), 14D10 ($n = 4$), or humanized anti-CD26 mAb ($n = 4$) on the 14th day after cancer cell inoculation when the tumor mass became visible (5 mm in size). Each mAb was given at 10 μ g per injection at thrice per week. **B**, representative resected specimens in s.c. tumorigenicity model on 35th day after first mAb treatment. **C**, effect of humanized anti-CD26 mAb in tumor dissemination model was evaluated. JMN cells (1×10^5) were injected i.v. into mice in each group. Mice were treated with i.v. injection of isotype-matched control mAb ($n = 4$), 5F8 ($n = 4$), 14D10 ($n = 4$), or humanized anti-CD26 mAb ($n = 4$) on the day of cancer cell injection. Each mAb was given at 10 μ g per injection at thrice per week.

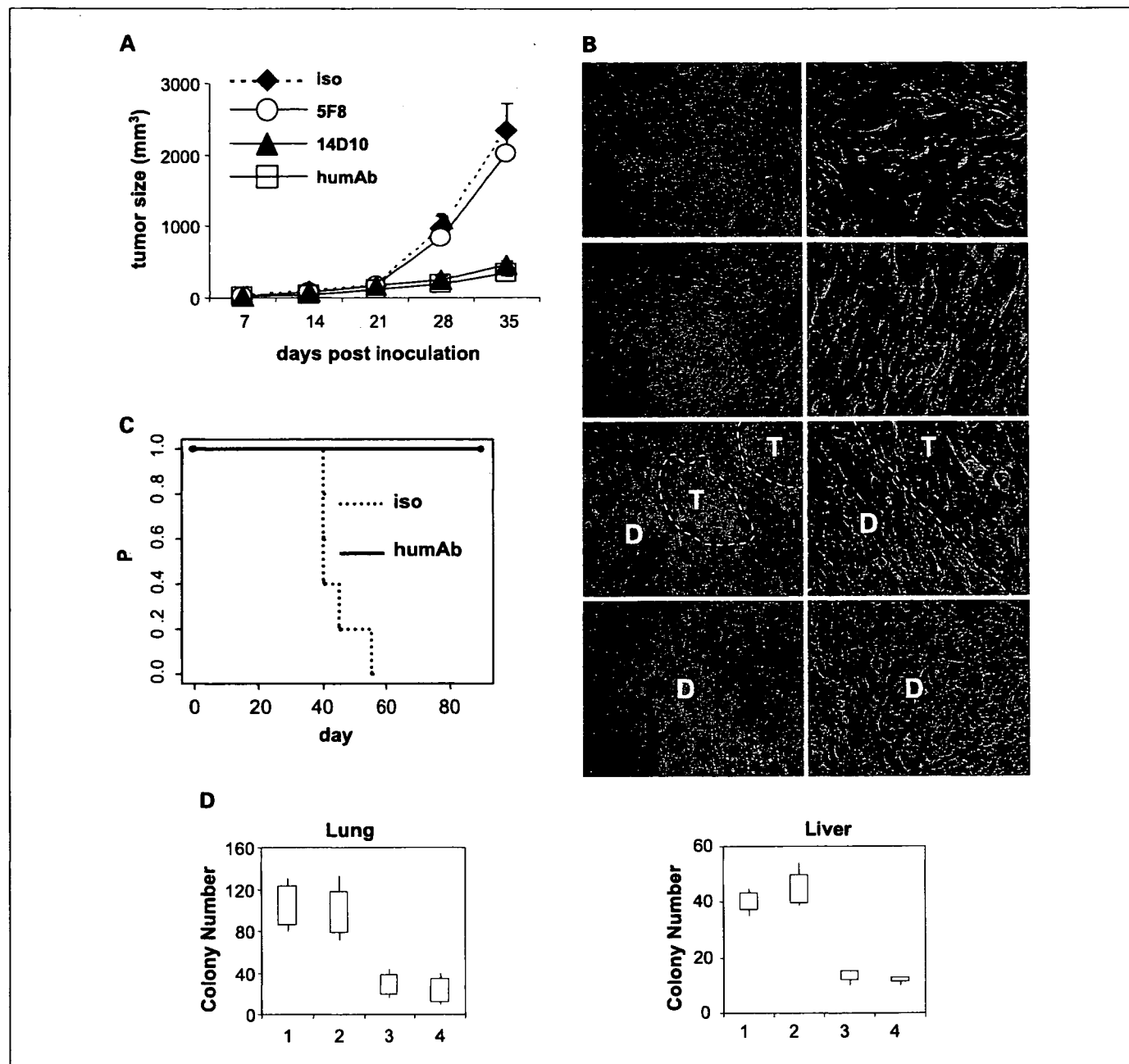


Fig. 5. *In vivo* direct and indirect effect of humanized anti-CD26 mAb; mouse ADCC presence model. Six-week-old female Balb mice were enrolled in this experiment. **A**, effect of humanized anti-CD26 mAb in s.c. tumorigenicity was evaluated. JMN cells (1×10^6) were inoculated s.c. into the left flank of mice. Mice were treated with intratumoral injection of isotype-matched control mAb ($n = 4$), 5F8 ($n = 4$), 14D10 ($n = 4$), or humanized anti-CD26 mAb ($n = 4$) on the 14th day after cancer cell inoculation when the tumor mass became visible (5 mm in size). Each mAb was given at 10 μ g per injection at thrice per week. **B**, representative H&E stain feature of resected specimens in s.c. tumorigenicity model on 35th day after first mAb treatment. *a*, isotype-matched control mAb ($\times 100$); *b*, isotype-matched control mAb ($\times 600$); *c*, 5F8 ($\times 100$); *d*, 5F8 ($\times 600$); *e*, 14D10 ($\times 100$); *f*, 14D10 ($\times 600$); *g*, humanized anti-CD26 mAb ($\times 100$); *h*, humanized anti-CD26 mAb ($\times 600$). White broken line, the line between tumor (T) and dead tissue (D). **C**, effect of humanized anti-CD26 mAb in tumor dissemination model was evaluated. JMN cells (1×10^5) were injected i.v. into mice in each group. Mice were treated with i.v. injection of isotype-matched control mAb ($n = 5$) or humanized anti-CD26 mAb ($n = 5$) on the day of cancer cell injection. Each mAb was given at 10 μ g per injection at thrice per week. **D**, effect of humanized anti-CD26 mAb onto distant metastasis formation in tumor dissemination model was evaluated. JMN cells (1×10^5) were injected i.v. into mice in each group. Mice were treated with i.v. injection of isotype-matched control mAb (lane 1, $n = 4$), 5F8 (lane 2, $n = 4$), 14D10 (lane 3, $n = 4$), or humanized anti-CD26 mAb (lane 4, $n = 4$) on the day of cancer cell injection. Each mAb was given at 10 μ g per injection at thrice per week. On 35th day after cancer cell injection, mice were euthanized and multiple metastasis formation in the lung and liver was calculated.

been previously reported that p27^{kip1} is up-regulated during contact inhibition (26).

Both humanized anti-CD26 mAb and 14D10 display direct inhibition of malignant mesothelioma growth via p27^{kip1} up-regulation and disruption of binding to ECM. Hence, our

results with these anti-CD26 monoclonal antibodies are consistent with those obtained from above small interfering RNA study, showing that both humanized anti-CD26 mAb and 14D10 have an antagonistic effect on the adhesive property of malignant mesothelioma.

Further examination of their effector functions associated with anti-CD26 mAb-mediated antitumor effect indicates that humanized anti-CD26 mAb, but 14D10, elicits ADCC-induced cell lysis. Cross-linking of humanized anti-CD26 mAb results in an accumulation of annexin V-positive and propidium iodide-positive population and cleavage of activated caspase-3. These data suggest that humanization of anti-CD26 mAb elicits greater contribution from ADCC in addition to a direct antitumor effect. Meanwhile, the precious reason why humanized anti-CD26 mAb does not induce CDC activity is not clear at the moment. One of the reasons is the high-surface expression of DAF and CD59, which are antagonistic to human complement proteins (data not shown). Or, our *in vitro* system may not be appropriate for the induction of CDC activation.

In vivo study with NOD-SCID mice shows that humanized anti-CD26 mAb and 14D10 reduce the tumorigenicity of s.c.-inoculated JMN cells, suggesting that humanized anti-CD26 mAb possesses direct antitumor effect as well. Our results also suggest that humanized anti-CD26 mAb is more potent in reducing tumor formation, possibly due to its higher binding affinity to CD26 than 14D10.

Meanwhile, *in vivo* study with Balb mice show that humanized anti-CD26 mAb and 14D10 are equally effective in reducing the tumorigenicity of s.c.-inoculated JMN cells. These data suggest that the mouse effector system may

potentiate the antitumor effect of 14D10 more than humanized anti-CD26 mAb. In fact, not only humanized anti-CD26 mAb but also 14D10-treated tumor specimens from these mice exhibit a reduction of viable cells in tumor mass. It is also noteworthy that both humanized anti-CD26 mAb and 14D10 reduce the formation of distant metastasis, findings which may be partly explained from our *in vitro* results that CD26 serves as a binding protein to distinct ECM proteins.

In vivo study with NOG-SCID mice which lack functional mice effectors show that dual-xenograft of HuEC plus target cells results in greater mouse survival than single xenograft of target cells when combined with humanized anti-CD26 mAb. These data clearly corroborate the *in vitro* data, suggesting that humanized anti-CD26 mAb induces a biphasic antitumor action with a human effector system.

CD26 status may be altered in cancer and may have an effect on the growth and metastatic potential of various tumors. Absence of CD26 is associated with the development of some cancers, whereas presence of CD26 is associated with a more aggressive phenotype in other neoplasms. For example, in non-small cell lung cancer cell lines, cells transfected with CD26 develop morphologic changes, altered contact inhibition, and reduced ability for anchorage-independent growth (29). CD26 reexpression also correlates with increased p21^{cip2/waf1} expression, leading to induction of apoptosis and cell cycle arrest in G₁ stage. Wesley et al. reported that CD26/dipeptidyl peptidase IV up-regulates the expression of CDK1 p27^{kip1} by 4-fold to 6-fold in CD26-transfected DU-145 metastatic prostate cancer cells compared with the parent and vector-transfected DU-145 cells (30). It is also reported that overexpression of CD26 in ovarian cancer leads to increased E-cadherin and tissue inhibitors of matrix metalloproteinases, resulting in decreased invasive potential (31). CD26/dipeptidyl peptidase IV thus functions as a tumor suppressor in the cases described above, and its down-regulation may contribute to the loss of growth control. In contrast, CD26 expression is associated with a more aggressive clinical course in T-cell large granular lymphocyte leukemia (32).

An earlier report indicated that CD26 and CD40L expression is mutually exclusive, with CD40L expressed on cells from more indolent diseases. Of note is that CD26 expression on T-cell LBL/ALL is associated with a worse survival (33). We now show that CD26 is highly expressed in malignant mesothelioma tissues and anti-CD26 mAb treatment and CD26 down-regulation by siRNA in CD26-positive malignant mesothelioma cell lines lead to contact inhibition and p27^{kip1} up-regulation. Therefore in case of malignant tumors, such as T-cell lymphoma, and malignant mesothelioma, CD26 plays a role in tumor growth and may be involved in invasion and metastasis.

Malignant mesothelioma is an aggressive neoplasm with a dismal prognosis and is relatively unresponsive to chemotherapy. One study systematically reviewed evidence for chemotherapy effect from 1965 through June 2001 and found 83 studies with 88 treatment arms (34). Cisplatin was the most active single drug, and cisplatin with doxorubicin had the highest response rate (28.5% response rate; confidence interval, 21.3% to 35.7%). Since this report, results of a phase III randomized trial (using 448 chemotherapy naive patients with unresectable mesothelioma) involving the combination cisplatin/pemetrexed (an antimetabolite) or cisplatin alone have shown that medium survival is extended from 9.3 months in

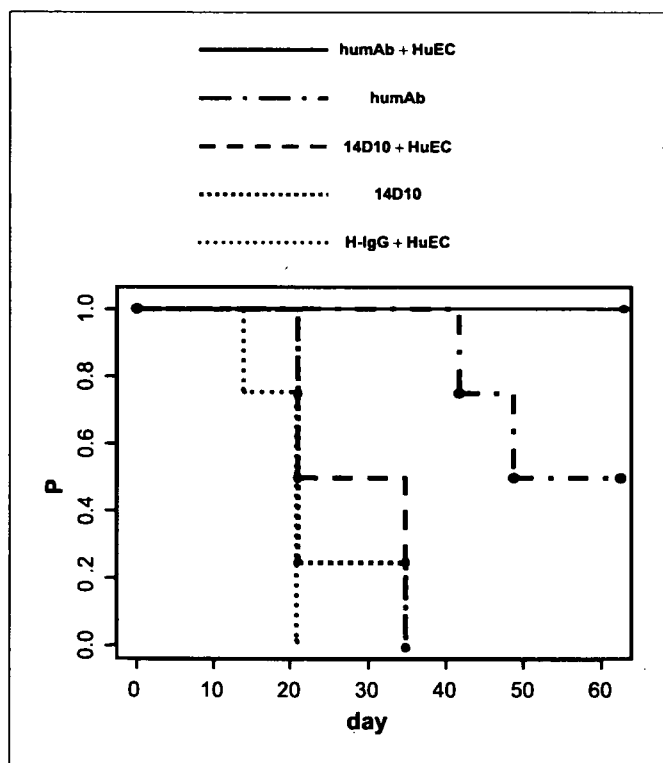


Fig. 6. *In vivo* direct and indirect effect of humanized anti-CD26 mAb: human ADCC presence model. Six-week-old female NOG-SCID mice were enrolled in this experiment. Mice were divided into two groups, HuECs-implanted group and HuEC-negative group, respectively. All mice were pretreated with anti- α -asialo-GM1 polyclonal antisera i.p. 2 d before HuEC implantation. HuEC were implanted i.p. with effector/target ratio of 10:1. JMN cells (1×10^6) were implanted 1 d after HuEC implantation into the peritoneal cavity of mice. The latter group was left untreated. All mice were treated with human normal IgG + HuEC (H-IgG+HuEC, $n = 4$), 14D10 ($n = 4$), 14D10 + HuEC ($n = 4$), humanized anti-CD26 mAb ($n = 4$), or humanized anti-CD26 mAb+HuEC (humAb+HuEC, $n = 4$). Each mAb was given i.p. at 10 μ g per injection, 1, 3, and 5 d after cancer cell implantation.

patients treated with cisplatin to 12.1 months in patients treated with both agents (35). However, standard treatments for malignant mesothelioma are still not satisfactory in terms of survival; hence, there is an urgent need for novel therapeutic approaches for malignant mesothelioma.

Our data therefore indicate that the novel humanized anti-CD26 mAb is an effective therapeutic tool for cancer treatment including malignant mesothelioma, as it can use the human effector system to target cancer cells in addition to its direct antitumor effect.

References

- Britton M. The epidemiology of mesothelioma. *Semin Surg Oncol* 2002;29:18–25.
- Connelly RR, Spirtas R, Myers MH, Percy CL, Fraumeni JF, Jr. Demographic patterns for mesothelioma in the United States. *J Natl Cancer Inst* 1987;78:1053–60.
- Ismaril-Khan R, Robinson LA, Williams CC, Jr., Garrett CR, Bepler G, Simon GR. Malignant Pleural Mesothelioma, a comprehensive review. *Cancer control* 2006;13:255–63.
- Pass H. Malignant pleural mesothelioma, surgical roles and novel therapies. *Clin Lung Cancer* 2001;3:102–17.
- Morimoto C, Schlossman SF. The structure and function of CD26 in the T-cell immune response. *Immunol Rev* 1998;161:55–70.
- Ishii T, Ohnuma K, Murakami A, et al. CD26-mediated signaling for T cell activation occurs in lipid rafts through its association with CD45RO. *Proc Natl Acad Sci U S A* 2001;98:12138–43.
- Ohnuma K, Yamochi T, Uchiyama M, et al. CD26 up-regulates expression of CD86 on antigen-presenting cells by means of caveolin-1. *Proc Natl Acad Sci U S A* 2004;101:14186–91.
- Yamochi T, Yamochi T, Aytac U, et al. Regulation of p38 phosphorylation and topoisomerase II α expression in the B-cell lymphoma line Jiyoye by CD26/dipeptidyl peptidase IV is associated with enhanced *in vitro* and *in vivo* sensitivity to doxorubicin. *Cancer Res* 2005;65:1973–83.
- Pro B, Dang NH. CD26/dipeptidyl peptidase IV and its role in cancer. *Histol Histopathol* 2004;19:1345–51.
- Iwata S, Morimoto C. CD26/dipeptidyl peptidase IV in context. The different roles of a multifunctional ectoenzyme in malignant transformation. *J Exp Med* 1999;190:301–6.
- Kehlen A, Lendeckel U, Dralle H, Langner J, Hoang-Vu C. Biological significance of aminopeptidase N/CD13 in thyroid carcinomas. *Cancer Res* 2003;63:8500–6.
- Kajiyama H, Kikkawa F, Suzuki T, Shibata K, Ino K, Mizutani S. Prolonged survival and decreased invasive activity attributable to dipeptidyl peptidase IV overexpression in ovarian carcinoma. *Cancer Res* 2002;62:2753–7.
- Cheng HC, Abdel-Ghany M, Pauli BU. A novel consensus motif in fibronectin mediates dipeptidyl peptidase IV adhesion and metastasis. *J Biol Chem* 2003;278:24600–7.
- Johnson RC, Zhu D, Augustin-Voss HG, Pauli BU. Lung endothelial dipeptidyl peptidase IV is an adhesion molecule for lung-metastatic rat breast and prostate carcinoma cells. *J Cell Biol* 1993;121:1423–32.
- Dang NH, Torimoto Y, Schlossman SF, Morimoto C. Human CD4 helper T cell activation: functional involvement of two distinct collagen receptors. *J Exp Med* 1990;172:649–52.
- Ohnuma K, Ishii T, Iwata S, et al. G₁-S cell cycle arrest provoked in human T cells by antibody to CD26. *Immunology* 2002;107:325–33.
- Ho L, Aytac U, Stephens LC, et al. *In vitro* and *in vivo* antitumor effect of the anti-CD26 monoclonal antibody 1F7 on human CD30+ anaplastic large cell T-cell lymphoma Karpas 299. *Clin Cancer Res* 2001;7:2031–40.
- Inamoto T, Yamochi T, Ohnuma K, et al. Anti-CD26 monoclonal antibody-mediated G₁-S arrest of human renal clear cell carcinoma Caki-2 is associated with retinoblastoma substrate dephosphorylation, cyclin-dependent kinase 2 reduction, p27(kip1) enhancement, and disruption of binding to the extracellular matrix. *Clin Cancer Res* 2006;12:3470–7.
- Usami N, Fukui T, Kondo M, et al. Establishment and characterization of four malignant pleural mesothelioma cell lines from Japanese patients. *Cancer Sci* 2006;97:387–94.
- Morimoto C, Torimoto Y, Levinson G, et al. 1F7, a novel cell surface molecule, involved in helper function of CD4 cells. *J Immunol* 1989;143:3430–9.
- Kobayashi S, Ohnuma K, Uchiyama M, et al. Association of CD26 with CD45RA outside lipid rafts attenuates cord blood T-cell activation. *Blood* 2004;103:1002–10.
- Tanaka J, Miwa Y, Miyoshi K, Ueno A, Inoue H. Construction of Epstein-Barr virus-based expression vector containing mini-oriP. *Biochem Biophys Res Commun* 1999;264:938–43.
- Sato K, Aytac U, Yamochi T, et al. CD26/dipeptidyl peptidase IV enhances expression of topoisomerase II α and sensitivity to apoptosis induced by topoisomerase II inhibitors. *Br J Cancer* 2003;89:1366–74.
- Prang N, Preithner S, Brischwein K, et al. Cellular and complement-dependent cytotoxicity of Ep-CAM-specific monoclonal antibody MT201 against breast cancer cell lines. *Br J Cancer* 2005;92:342–9.
- Dang NH, Torimoto Y, Schlossman SF, Morimoto C. Human CD4 helper T cell activation: functional involvement of two distinct collagen receptors, 1F7 and VLA integrin family. *J Exp Med* 1990;172:649–52.
- Suzuki E, Nagata D, Yoshizumi M, et al. Reentry into the cell cycle of contact-inhibited vascular endothelial cells by a phosphatase inhibitor. Possible involvement of extracellular signal-regulated kinase and phosphatidylinositol 3-kinase. *J Biol Chem* 2000;275:3637–44.
- Levenberg S, Yarden A, Kam Z, Geiger B. p27 is involved in N-cadherin-mediated contact inhibition of cell growth and S-phase entry. *Oncogene* 1999;18:869–76.
- Shultz LD, Schweitzer PA, Christianson SW, et al. Multiple defects in innate and adaptive immunologic function in NOD/LtSz-scid mice. *J Immunol* 1995;154:180–91.
- Wesley UV, Tiwari S, Hoghton AN. Role for dipeptidyl peptidase in tumor suppression of human non small cell lung carcinoma cells (NSCLC). *Int J Cancer* 2004;109:855–66.
- Wesley UV, McGroarty M, Homoyouni A. Dipeptidyl peptidase inhibits malignant phenotype of prostate cancer cells by blocking basic fibroblast growth factor signaling pathway. *Cancer Res* 2005;65:1325–34.
- Kajiyama H, Kikkawa F, Khin E, Shibata K, Ino K, Mizutani S. Dipeptidyl peptidase overexpression induces up-regulation of E-cadherin and tissue inhibitors of matrix metalloproteinases, resulting in decreased invasive potential in ovarian carcinoma cells. *Cancer Res* 2003;63:2278–83.
- Dang NH, Aytac U, Sato K, et al. T-large granular lymphocyte lymphoproliferative disorder: expression of CD26 as a marker of clinically aggressive disease and characterization of marrow inhibition. *Br J Haematol* 2003;121:857–65.
- Canbon A, Gloghini A, Zagonel V, et al. The expression of CD26 and CD40 ligand is mutually exclusive in human T-cell non-Hodgkin's lymphomas/leukemias. *Blood* 1995;86:4617–26.
- Berghmans T, Paesmans M, Lalami Y, et al. Activity of chemotherapy and immunotherapy on malignant mesothelioma: a systemic review of the literature with meta-analysis. *Lung Cancer* 2002;38:111–21.
- Vogelzang NJ, Rusthoven JJ, Symanowski J, et al. Phase study of pemetrexed in combination with cisplatin versus cisplatin alone in patients with malignant pleural mesothelioma. *J Clin Oncol* 2003;21:2629–30.

Transcriptional Up-regulation of Inhibitory PAS Domain Protein Gene Expression by Hypoxia-inducible Factor 1 (HIF-1)

A NEGATIVE FEEDBACK REGULATORY CIRCUIT IN HIF-1-MEDIATED SIGNALING IN HYPOXIC CELLS*

Received for publication, January 25, 2007, and in revised form, March 12, 2007. Published, JBC Papers in Press, March 12, 2007, DOI 10.1074/jbc.M700732200

Yuichi Makino^{†§¶1}, Rie Uenishi[¶], Kensaku Okamoto[§], Tsubasa Isoe[§], Osamu Hosono[‡], Hirotohi Tanaka[‡], Arvydas Kanopka^{||}, Lorenz Poellinger^{**}, Masakazu Haneda[§], and Chikao Morimoto[‡]

From the [‡]Division of Clinical Immunology, Advanced Clinical Research Center, Institute of Medical Science, University of Tokyo, 4-6-1, Shirokanedai, Minato-ku, Tokyo 108-8639, Japan, the [§]Section of Metabolism and Biosystemic Science, Department of Internal Medicine, Asahikawa Medical College, 2-1 Midorigaoka-higashi, Asahikawa, 078-8510, Japan, [¶]PRESTO, Japan Science and Technology Agency, 4-1-8 Honchou, Kawaguchi, Saitama 332-0012, Japan, and the ^{||}Institute of Biotechnology, Graiciuno 8, 2028 Vilnius, Lithuania and the ^{**}Department of Cell and Molecular Biology, Medical Nobel Institute, Karolinska Institute, S-171 77 Stockholm, Sweden

The inhibitory PAS (Per/Arnt/Sim) domain protein (IPAS), a dominant negative regulator of hypoxia-inducible transcription factors (HIFs), is potentially implicated in negative regulation of angiogenesis in such tissues as the avascular cornea of the eye. We have previously shown IPAS mRNA expression is up-regulated in hypoxic tissues, which at least in part involves hypoxia-dependent alternative splicing of the transcripts from the IPAS/HIF-3 α locus. In the present study, we demonstrate that a hypoxia-driven transcriptional mechanism also plays a role in augmentation of IPAS gene expression. Isolation and analyses of the promoter region flanking to the first exon of IPAS gene revealed a functional hypoxia response element at position -834 to -799, whereas the sequence upstream of the HIF-3 α first exon scarcely responded to hypoxic stimuli. A transient transfection experiment demonstrated that HIF-1 α mediates IPAS promoter activation via the functional hypoxia response element under hypoxic conditions and that a constitutively active form of HIF-1 α is sufficient for induction of the promoter in normoxic cells. Moreover, chromatin immunoprecipitation and electrophoretic mobility shift assays showed binding of the HIF-1 complex to the element in a hypoxia-dependent manner. Taken together, HIF-1 directly up-regulates IPAS gene expression through a mechanism distinct from RNA splicing, providing a further level of negative feedback gene regulation in adaptive responses to hypoxic/ischemic conditions.

Cellular adaptation to hypoxic conditions is accompanied by changes in expression of a panel of genes encoding physiologi-

cally relevant proteins (1–3). These genes have been shown to contain hypoxia response elements (HREs)² in their promoter regions. Under hypoxic conditions the response elements are recognized by a hypoxia-inducible transcription factor (HIF)-1, a heterodimeric complex of the basic helix-loop-helix PAS (Per/Arnt/Sim) domain proteins HIF-1 α and HIF-1 β (Arnt) (4). In addition, the HIF-1 α paralogs HIF-2 α (5, 6) and HIF-3 α (7) dimerize with Arnt in hypoxic cells to form DNA-binding complexes. Two distinct mechanisms are important for regulation of HIF-1 α and HIF-2 α activity by oxygen. Under normoxic conditions, HIF- α is targeted by the von Hippel-Lindau protein (pVHL) for ubiquitylation and rapid proteasomal degradation (8, 9). pVHL binding is mediated through hydroxylation of specific prolyl residues located in the central region of HIF- α proteins. Hydroxylation at the 4-position of those prolines of HIF- α enables formation of two hydrogen bonds to pVHL and increases the binding of pVHL to HIF- α by several orders of magnitude (10). This post-translational modification of HIF- α is catalyzed by HIF-prolyl hydroxylases, a set of dioxygenases that require O₂, Fe(II), and 2-oxoglutarate as cosubstrates. At low oxygen levels, there is a corresponding decrease in prolyl hydroxylation of HIF- α , resulting in release of pVHL and stabilization of HIF- α protein (11, 12). Stabilized HIF- α then translocates to the nucleus where it dimerizes with Arnt to bind to the HREs of target genes (13). Recently, a similar mode of regulation of HIF-3 α at the protein expression level has been suggested (14).

In addition to stabilization of HIF- α protein levels, hypoxia induces the function of the transactivation domains of HIF- α proteins and enhances their ability to interact with transcriptional coactivator proteins (5, 15, 16). Under normoxic conditions this interaction is blocked by hydroxylation of a conserved

* This work was supported by Grant-in-Aid for scientific research from the Ministry of Education, Culture, Sports, Science and Technology (to Y. M. and C. M.) and from PRESTO, the Japan Science and Technology Agency (To Y. M.). The costs of publication of this article were defrayed in part by the payment of page charges. This article must therefore be hereby marked "advertisement" in accordance with 18 U.S.C. Section 1734 solely to indicate this fact.

[†] To whom correspondence should be addressed: Section of Metabolism and Biosystemic Science, Dept. of Internal Medicine, Asahikawa Medical College, 2-1 Midorigaoka-higashi, Asahikawa 078-8510, Japan. Tel.: 81-166-68-2454; Fax: 81-166-68-2459; E-mail: makino@asahikawa-med.ac.jp.

² The abbreviations used are: HRE, hypoxia response element; IPAS, inhibitory PAS domain protein; HIF, hypoxia-inducible factor; Arnt, arylhydrocarbon receptor nuclear translocator; VEGF, vascular endothelial growth factor; MBEC, mouse brain endothelial cell(s); EMSA, electrophoretic mobility shift assay; Epo, erythropoietin; HBS, HIF-1-binding site; CMV, cytomegalovirus; RT, reverse transcription; PGC-1, peroxisome proliferator-activated receptor γ coactivator-1; ChIP, chromatin immunoprecipitation; PBS, phosphate-buffered saline; nt, nucleotide(s).